Nationaal Lucht- en Ruimtevaartlaboratorium
National Aerospace Laboratory NLR

Executive summary

Optimal Autorotation With Obstacle Avoidance For A Small-Scale Flybarless Helicopter UAV

Problem area
We derive optimal autorotative landing trajectories, for the case of a small-scale helicopter Unmanned Aerial Vehicle (UAV).

Description of work
These open-loop optimal trajectories represent the solution to the minimization of a cost objective, given system dynamics, controls and states equality and inequality constraints. The plant dynamics features a 3-D nonlinear helicopter model, including dynamics from the rigid body, the main rotor Revolutions Per Minute (RPM), and the actuators.

Results and conclusions
In this paper**,** we extend our previous results on optimal autorotation, and present an improved cost functional which, during the flight, maximizes helicopter performance and control smoothness, while minimizing roll-yaw cross-coupling. Further, we compute the Height-Velocity (H-V) diagram, and we include a novel obstacle avoidance capability. Finally, we conclude by a discussion of several simulation examples.

Applicability
Development of flight control systems for small-scale UAV helicopters.

Report no.
NLR-TP-2013-295

Author(s)
S. Taamallah

Report classification
UNCLASSIFIED

Date
July 2013

Knowledge area(s)
Helikoptertechnologie

Descriptor(s)
Unmanned Aerial Vehicle (UAV)
Helicopter Optimal Autorotation
Obstacle Avoidance

This report is based on a presentation held at the AIAA Guidance, Navigation, and Control Conference 13 - 16 August 2012, Minneapolis, Minnesota.

Optimal Autorotation With Obstacle Avoidance For A Small-Scale Flybarless Helicopter UAV

Nationaal Lucht- en Ruimtevaartlaboratorium, National Aerospace Laboratory NLR

Anthony Fokkerweg 2, 1059 CM Amsterdam,
P.O. Box 90502, 1006 BM Amsterdam, The Netherlands
Telephone +31 88 511 31 13, Fax +31 88 511 32 10, Web site: www.nlr.nl

Nationaal Lucht- en Ruimtevaartlaboratorium
National Aerospace Laboratory NLR

provisional issue
NLR-TP-2013-295

Optimal Autorotation With Obstacle Avoidance For A Small-Scale Flybarless Helicopter UAV

S. Taamallah

This report is based on a presentation held at the AIAA Guidance, Navigation, and Control Conference 13 - 16 August 2012, Minneapolis, Minnesota.

Customer	National Aerospace Laboratory NLR
Contract number	----
Owner	NLR
Division NLR	Aerospace Systems and Applications
Distribution	Limited
Classification of title	Unclassified
	July 2013

Approved by:

Author	Reviewer	Managing department
Date:	Date:	Date:

Contents

Nomrnclature 5

I. Introduction 5

I.A. Background 6

II. Helicopter Modeling Considerations 7

III. Control Architecture 9

IV. Optimal Trajectory 10

IV.A. State And Input Vectors 11

IV.B. Cost Functional

IV.C. Boumdary Conditions 11

IV.D. Trajectory Contrants 12

V. Obstacle Avoidance 13

VI. Direct Optimal Control and The Pseudospectral Discretization 14

VII. Simulation Results 15

VII.A. The Height-Velocity Diagram 16

VII.B. Optimal Autorotation 17

VIII. Discussion 22

IX. Conclusion 23

References 24

This page is intentionally left blank.

Optimal Autorotation With Obstacle Avoidance For A Small-Scale Flybarless Helicopter UAV

Skander Taamallah*†

National Aerospace Laboratory (NLR), 1059CM Amsterdam, The Netherlands

We derive optimal autorotative landing trajectories, for the case of a small-scale helicopter Unmanned Aerial Vehicle (UAV). These open-loop optimal trajectories represent the solution to the minimization of a cost objective, given system dynamics, controls and states equality and inequality constraints. The plant dynamics features a 3-D nonlinear helicopter model, including dynamics from the rigid body, the main rotor Revolutions Per Minute (RPM), and the actuators. In this paper, we extend our previous results on optimal autorotation, and present an improved cost functional which, during the flight, maximizes helicopter performance and control smoothness, while minimizing roll-yaw cross-coupling. Further, we compute the Height-Velocity (H-V) diagram, and we include a novel obstacle avoidance capability. Finally, we conclude by a discussion of several simulation examples.

Nomenclature

(x_N, x_E, x_Z)	3-D position of the vehicle Center of Gravity (CG), in inertial frame F_I, This frame is given by (x_I, y_I, z_I), see figure 2
(V_N, V_E, V_Z)	Inertial velocities of vehicle CG in frame F_I
(ϕ, θ, ψ)	vehicle angular orientations in roll-pitch-yaw respectively, with respect to F_I
(u, v, w)	CG linear velocities, with respect to F_I, and projected in the helicopter body frame F_b This frame is given by (x_b, y_b, z_b), see figure 2
(p, q, r)	CG rotational velocities, with respect to F_I, and projected in the helicopter body frame F_b
Ω_{MR}	Main Rotor (MR) angular velocity, also called MR Revolutions Per Minute (RPM)
$\Omega_{MR_{100\%}}$	Nominal MR (100%) angular velocity
θ_0	MR blade collective pitch
θ_{TR}	Tail Rotor (TR) blade collective pitch
θ_{1c}	MR blade lateral cyclic pitch
θ_{1s}	MR blade longitudinal cyclic pitch
(x_{TR}, y_{TR}, z_{TR})	TR hub coordinates in frame F_b
$R_{rot_{TR}}$	TR radius
$x_{Z_{TRBT}}$	Z-coordinate of tail rotor blade tip in frame F_I
z_o	Initial value of an element z
z_f	Final value of an element z

I. Introduction

Helicopter power-off flight, or autorotation, is a condition in which no power plant torque is applied to the main and tail rotors, a flight condition which is somewhat comparable to gliding for a fixed-wing aircraft. During an autorotation, the main rotor is not driven by a running engine, but by air flowing through the rotor disk bottom-up, while the helicopter is descending.[1] In this case, the power required to keep the rotor spinning is obtained from the vehicle's potential and kinetic energy. Now, an autorotative flight is

*R&D Engineer, Aircraft Systems Department, National Aerospace Laboratory (NLR), 1059CM Amsterdam, The Netherlands.

†Ph.D. Student, Delft Center for Systems and Control (DCSC), Faculty of Mechanical, Maritime and Materials Engineering, Delft University of Technology, 2628CD Delft, The Netherlands.

started when the engine fails on a single-engine helicopter, or when a tail rotor failure requires engine shut down. Unfortunately autorotation is a risky maneuver when performed on a manned helicopter, it requires indeed a good deal of training, if disaster is to be avoided. Additionally, quick reaction and critically timed control inputs are required for a safe autorotative landing,[2–4] since it is well known that a delayed or improperly performed autorotation can turn an incident into an accident or fatality.[5] For instance, a 1980 statistics[6] showed that at least 27% of all emergency autorotations involving the AH-1, UH-1, OH-58, and OH-6 helicopters resulted in some degree of vehicle damage or personnel injury, whereas a 1998 study[5] also highlighted that helicopter autorotation accounted for 7% of 1852 helicopter accidents. Such findings are somewhat disconcerting since autorotation ought to be the approved response to an emergency, rather than an emergency itself.[7] Further, it was also claimed that both the U.S. Army and Air Force have stopped performing autorotation training, after studies have shown that there were more injuries and aircraft damage from practicing autorotation than from autorotations required by actual engine failures.[7] Now, on the civilian side, it is as well known that autorotation training in a simulator occurs infrequently, since most simulators poorly reproduce the cues required for an autorotative flight.[4]

For the case of manned helicopters, the elements presented here-above plead for either (i) the availability of an automated autorotation safety system, that could land the vehicle once a power plant or tail rotor failure has been detected,[8] or (ii) for the availability of control guidance cues, that would assist a pilot in performing the maneuver.[9,10] Additionally, an automated autorotation system could potentially represent an alternative to multiple engine helicopter configurations,[8] as a safeguard against catastrophic engine failure. By eliminating the need for multi-engine helicopters, the availability of such a system would obviously translate into substantial cost savings, especially since it is well known that helicopter purchase price is more sensitive to installed power than to empty weight.[11]

For the case of unmanned helicopters, such an automated autorotation safety system would represent a substantial improvement towards helicopter UAV certification for the civilian airspace. Indeed the civil helicopter UAV market, primarily driven by security needs such as law enforcement and fire and rescue agencies, is currently only slowly developing, as system safety, airworthiness, and air-space integration issues still play a crucial role in the development and operation of these UAVs.[12]

In this paper we focus on the helicopter UAV case, with application to a small-scale flybarless helicopter, i.e. without a Bell-Hiller stabilizing bar. We extend our previous results on optimal autorotation,[13] and present the initial steps towards the design of such an automated autorotation safety system. Here, our goal is to find the optimal autorotative trajectories, subject to system and environment constraints, by maximizing flight performance and control smoothness, while minimizing dynamical cross-coupling effects. Hence, for a range of initial conditions for which feasible solutions do exist, i.e. in the form of safe landing, optimal autorotative trajectories can be computed off-line by a Trajectory Planner (TP), and stored as lookup tables, on-board a flight control computer. By so doing, these trajectories provide both the optimal states to be tracked by a feedback Trajectory Tracker (TT), and the feedforward nominal controls needed to track the trajectory. In this paper, we present the design of such a TP, in the case of a continuous-time, deterministic, nonlinear, and constrained framework; solved through a direct optimal control method. Here, the continuous-time formulation is first discretized, using a pseudospectral numerical scheme,[14–17] known to provide exponential convergence, provided the functions under considerations are sufficiently smooth. Pseudospectral techniques have widely been used in space and launch/reentry applications. However, they have so far only seen limited use in other aeronautical or (helicopter) UAV applications. Next, our problem is transcribed to a NonLinear Programming problem (NLP),[18–20] and this latter is solved numerically by a well known and efficient optimization technique, in our case a Sequential Quadratic Programming (SQP)[21–23] method.

I.A. Background

Over the last four decades, researchers have addressed the optimal autorotative flight problem through several optimization techniques. We start by mentioning the successful autorotative flight demonstration in the case of a small-scale helicopter, through the use of an apprenticeship learning method[24] in Ref. 25,26. Other approaches have also focused upon reinforcement learning in Ref. 27, and fuzzy-logic concepts in Ref. 28. Next, for the case of first principles based models, we briefly review the different optimization strategies that

have been researched. Indirect optimal control methods have been used in Ref. 29–34, whereas direct optimal control methods have been explored in Ref. 2, 3, 9, 35–44. Aside from these optimal control strategies, three other methods have also been investigated: (i) a nonlinear, neural network augmented, model-predictive control method in Ref. 45, (ii) a parameter optimization scheme, repeatedly solved, to find a backwards reachable set leading to safe landing in Ref. 46, and (iii) a parameter optimization scheme generating segmented routes, selecting a sequence of straight lines and curves in Ref. 47, 48. It is probably safe to state that the most natural framework for addressing trajectory planning problems is through optimal control theory.[49] Besides, any strategy that does not rely on the combined use of both realistic 3-D first principles based models, and optimal control, results at best in sub-optimal solutions, since the full dynamics of the vehicle are neither exploited from a vehicle flight performance viewpoint, nor from a control-optimization viewpoint.[50,51] Further, for the definition of the cost functional, most of the here-above listed contributions have focused solely upon the minimization of vehicle kinetic energy at the instant of touch-down. Some have also considered using a running cost over time, which includes criteria involving either (i) the minimization of control rates,[3,37,38,43] or (ii) the minimization of main rotor RPM deviations from its nominal value, while limiting the excessive build-up of vehicle kinetic energy during the descent.[34,40] None of the previous results have considered the definition of a cost functional that includes all of these criteria, with the additional minimization of vehicle sidewards flight, and roll/pitch rates, while maximizing flight into the wind. Indeed, this represents the first contribution of our paper. The second is the inclusion of an obstacle avoidance capability. Finally, we apply a pseudospectral discretization scheme, in a direct method, to solve the autorotation nonlinear optimal control problem.

The remainder of the paper is organized as follows. In Section II, helicopter model fidelity aspects are discussed. In Section III, the control architecture is outlined. In Section IV, the general case optimal control problem is defined. In Section V, the obstacle avoidance functionality is given. In Section VI, direct optimal control and the pseudospectral method are reviewed. In Section VII, simulation results are analyzed. In Section VIII, a discussion of the results is adjoined. Finally, conclusions and future directions are presented in Section IX.

II. Helicopter Modeling Considerations

Given that most nonlinear constrained optimization problems are typically either computationally intensive (real-time computation), or memory intensive (off-line computation), solving the optimization problem in the full vehicle state space (including higher-order main rotor modes) is in general computationally intractable,[37] and hence for trajectory planning, a simplified dynamical model becomes necessary. Accordingly, this brings upfront the question of model fidelity. Here, several model classifications exist. In particular, a well-established approach, based on rotor modeling requirements derived from their area of application and flight envelope ranges, is given in Ref. 52. However, in this paper, we present a simpler classification, specifically tailored for small-scale helicopter UAVs, which contains three model classes, see table 1.

Model Sophistication	Class I	Class II	Class III
Model Dynamics	Simple	Simple	High-Fidelity
Model Validity	Simple	High-Fidelity	High-Fidelity

Table 1. Model classes

According to Ref. 53 the level of model sophistication, to conveniently describe model complexity, may be formulated by two factors, namely *model dynamics* and *model validity*, defined as:

- *Model dynamics.* It qualifies the level of detail in representing the dynamics of the helicopter. This factor determines the validity of the model in terms of the frequency range of applicability. In table 1, the qualificative *simple* refers to 2-D or 3-D models having rigid-body, actuators, and main rotor Revolutions Per Minute (RPM) dynamics, while the qualification *high-fidelity* refers to helicopter models that also include the main rotor higher-order phenomena, such as blade flap-lag and rotor inflow dynamics.

- *Model validity*. It represents the level of sophistication in calculating the helicopter forces, moments, etc. This factor determines the domain of validity in the flight envelope. In table 1, the qualificative *simple* refers to models that crudely reproduce the associated laws of physics, while the qualification *high-fidelity* refers to models that accurately simulate the vehicle forces and moments, including at high speed flight, descending in the Vortex-Ring-State (VRS), and the autorotation condition.[1]

A helicopter has four independent control inputs, it is thus a classical example of a so-called under-actuated system, since the number of control inputs is smaller than the dimension of its associated six-dimensional manifold Q, i.e. the vehicle configuration manifold. A vehicle *configuration* $\{q|q \in Q\}$ identifies the position of all of its points with respect to an inertial frame, while a *configuration manifold* represents the set of all possible vehicle configurations. Further, a helicopter has also nonholomonic constraints,[54–56] defined as a non-integrable constraint of the form $\eta(q, \dot{q}, \ddot{q}) = 0$, due to the coupling between its rotational and the translational motions.[57] These aspects are mentioned here since they play a primary role in constrained control techniques, designed to serve trajectory following systems.[58]

Now, models belonging to class I undeniably shorten the software development process, allow for computationally tractable simulations, and provide both valuable qualitative and quantitative insights into the optimal autorotative flight problem and its associated Height-Velocity (H-V) diagram (see Section VII.A). For all their benefits, these simplified models have several liabilities. To start, it is obvious that the fidelity of any simulation predictions, analysis thereof, and corresponding conclusions, crucially hinge upon the fidelity of the vehicle model. Indeed, trajectories predicted with oversimplified models might exhibit significant discrepancies with flight data.[42] The issue of performance is of relevance here, since it is well known that approximate representations of the *model dynamics* may result in sub-optimal solutions and conservative performance results.[59] Second, and beyond any (benign) discrepancy matters, comes the crucial issue of feasibility, since it is long known that generated optimal trajectories based on simple *model validity*, that ignore the nonholomonic constraints, may not be feasible.[60,61] Third, the issue of feedforward control inputs computed from the TP compensator, see figure 1, comes into play since these inputs are known to be highly sensitive to model class type and associated uncertainties.[62,63] Finally, in case the control architecture also includes a TT keeping the vehicle flying in the neighborhood of the computed optimal trajectory, we also have to consider the TT real-time computational aspects, since the lower the fidelity of the model used during the trajectory generation process, the higher the demand and effort on real-time feedback computation.[64,65]

On the other hand, comprehensive models belonging to class III, with high-fidelity *model dynamics* and high-fidelity *model validity*, allow for the design of optimal trajectories that capture the fine-scale helicopter higher frequency phenomena, such as the main rotor blade flap-lag dynamics,[66] and main rotor dynamic inflow,[67,68] resulting in highly accurate trajectories. The two main drawbacks of using such models come from (i) the inherent numerical instabilities associated with the numerical optimizations, that tend to get exacerbated with the increase in model complexity, and (ii) the corresponding (very) high computational cost, which may effectively preclude any further potential on-line use of the trajectory generation process, for real-time re-planning applications, albeit in a receding-horizon framework.

Now models belonging to class II, having simplified *model dynamics* and high-fidelity *model validity*, may provide a well-balanced approach.[63] Here, the model dynamics typically includes the rigid-body equations of motions, the main rotor RPM, and the actuator dynamics, while the higher-order main rotor phenomena are modeled by their corresponding steady-state expressions. Indeed, the bandwidth of the neglected dynamics is generally higher than the bandwidth of vehicle flight mechanics, and higher than any flight mechanics closed-loop controller bandwidth. Hence, and on the grounds of this time-scale separation principle,[69] the lack of high frequency modeling detail becomes typically justifiable and acceptable for flight mechanics applications.[37] The obvious advantage here is great computational savings, with a minimal loss in accuracy and fidelity.

With this in mind, and for the derivation of the optimal autorotative trajectories, we chose to use a typical example of a first principles based class II model structure. This represents an additional specificity of our work. Indeed, the focus of previous research[a] has either relied upon 2-D class I models,[2,3,9,29–37,39,44–46]

[a] For the case of Ref. 40, the model used was not published in the open English literature

3-D class I models,[47,48] or 3-D class III models[38,42,43] such as Flightlab®.[70] The helicopter model used in this paper is based on a simplified version of the work reported in Ref. 71, 72. The model reproduces the flight dynamics of a flybarless small-scale helicopter UAV, having an articulated Pitch-Lag-Flap (P-L-F) main rotor with rigid blades, for both ClockWise (CW) and Counter-ClockWise (CCW) main rotor rotation. This nonlinear model includes the twelve-states rigid body equations of motion, and the single-state main rotor Revolutions Per Minute (RPM). Additionally, it features the main rotor static Tip-Path-Plane (TPP) motion,[73,74] and the static uniform inflow component.[67,75] Further, static ground effect has been accounted for by a correction factor applied to the non-dimensional total velocity at the rotor disk center.[76] Main rotor forces and moments are given as closed-form expressions derived from Ref. 77, while the tail rotor is modeled as a Bailey type rotor.[78] The fuselage model is based upon aerodynamic lift and drag coefficients, which are tabulated as a function of airflow angle of attack and sideslip angles. These lookup tables are derived from a scaled-down full-size helicopter fuselage aerodynamic model. The horizontal and vertical tail models are based upon flat-plate aerodynamic lift and drag coefficients, tabulated as a function of airflow angle of attack and Mach number. Finally, deterministic wind and Dryden stochastic gust velocities may also be added. The model is valid for stability and control investigations up to an advance ratio limit of about 0.3,[73,74,79] which is beyond the flight envelope of this small-scale helicopter. Finally, this model is also applicable for flight in the Vortex-Ring-State (VRS)[80] and autorotation.[1] Our complete model is further presented in detail in Ref. 81.

III. Control Architecture

We present next a control architecture, for an automated autorotation safety system, see figure 1. We make use of the linear control theory standard two-degree of freedom controller design paradigm,[62] in which the philosophy decouples the TP, i.e. a feedforward compensator, from the asymptotic TT problem, i.e. a feedback compensator. The role of the TP is to generate a feasible and optimal trajectory reference $\mathbf{X_{ref}}$, for the helicopter to follow, and additionally, though not necessarily, the feedforward nominal control inputs $\mathbf{U_{ref}}$, needed to track this trajectory. Feedforward control may indeed be added to improve disturbance rejection, and the tracking performance, particularly at frequencies where feedback is not effective.[62] This should be done with care, since it is well known that feedforward control is sensitive to model uncertainty.

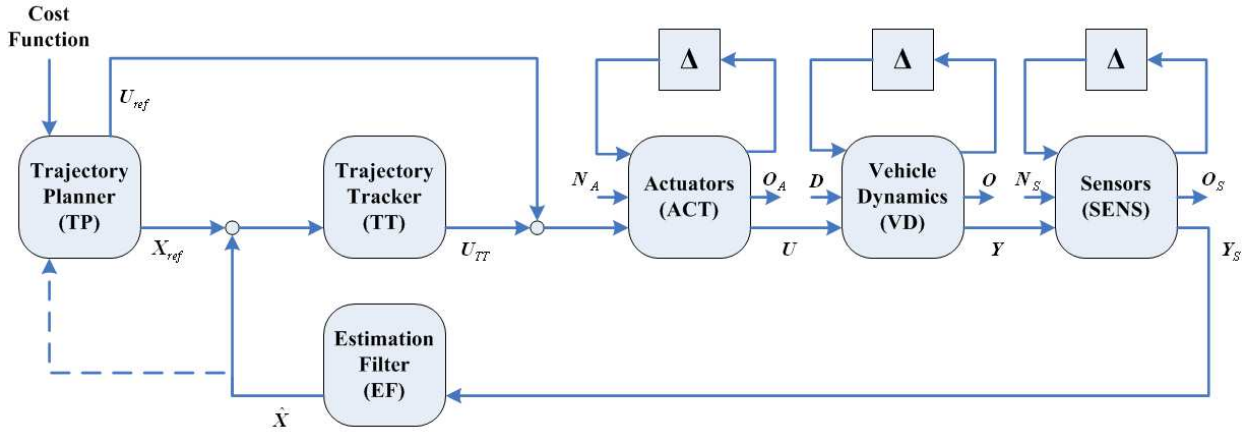

Figure 1. Control architecture

The TP computes off-line an open-loop optimal trajectory, given a cost objective, system dynamics, and controls and states equality and inequality constraints. On the other hand, The TT compares current estimated state values $\hat{\mathbf{X}}$ with the reference values produced by the TP, and formulates the feedback controls $\mathbf{U_{TT}}$ aimed at decreasing this tracking error. This latter may be due to a combination of model uncertainty (unmodeled higher-order dynamics, unmodeled static nonlinearities, parametric uncertainties, delays), and signal uncertainty (wind disturbances and noise). The additional feedback path, denoted by a dashed line, allows for updating the generated trajectory based upon the current estimated state. This results in a closed-

loop calculation of the reference trajectory, which may only be feasible in case the TP is capable of real-time computation[b]. In our current system implementation, which does not rely upon receding-horizon TP formulations, computational capabilities and software limitations prevent the calculation of the TP solutions from being recomputed in real-time, hence we will not have feedback into the TP box. Separating the trajectory generation and stabilization phases, although being a sub-optimal approach, offers the advantage of effectively exploiting the geometric nature of the system to generate trajectories, while also making use of the linear structure of the error dynamics.[82] We can then treat the system nonlinearities separately from the problem of robust stabilization and disturbance rejection. Indeed, the analysis and synthesis of gain-scheduled H_∞ methods, or the more modern Linear Parameter Varying (LPV) and receding horizon methods are particularly well-suited within this separation context. The other components of figure 1 include the Estimation Filter (EF), which estimates the vehicle state and wind field components, together with scale factor, bias errors, and noise inherent to low-cost sensors. The Vehicle Dynamics (VD) provides a descriptive model of the helicopter. Further, N_A and N_S represent input noise signals, D an input disturbance, U the vehicle input signal, O, O_A, O_S, Y, Y_S output signals, and Δ an uncertainty. Now, since the focus of this paper is on optimal autorotative trajectories, we elaborate in the sequel on the TP design. The VD is presented in Ref. 81, while the TT and EF components will be presented in future publications.

IV. Optimal Trajectory

We consider the following problem, consisting in minimizing the Bolza cost functional $J(\mathbf{x}(t), \mathbf{u}(t), T_o, T_f)$, with the state-vector $\mathbf{x}(t)$, and control input $\mathbf{u}(t)$, both defined on compact sets $\mathbf{x}(t) \in \mathcal{X}(t) \subseteq \mathbb{R}^{n_x}$, $\mathbf{u}(t) \in \mathcal{U}(t, \mathbf{x}(t)) \subseteq \mathbb{R}^{n_u}$, denoting the feasible state and control spaces respectively. Here, for the purpose of generality, the control set $\mathcal{U}(t, \mathbf{x}(t))$ is allowed to be state-dependent to accommodate for considerations of aerospace applications. Further, the independent time variable t is defined over the time domain $\Omega = (T_o, T_f)$, where the final time T_f may be free or fixed. We have

$$\begin{aligned} J(\mathbf{x}(t), \mathbf{u}(t), T_o, T_f) \quad &\triangleq \Phi(\mathbf{x}(T_o), T_o, \mathbf{x}(T_f), T_f) \\ &+ \int_\Omega \Psi(\mathbf{x}(t), \mathbf{u}(t), t) dt \end{aligned} \tag{1}$$

In the general problem formulation, the cost functional $J(.)$ has contributions from a fixed cost $\Phi(.)$, and a running cost over time $\int_\Omega \Psi(.)dt$. Additionally, this cost functional $J(.)$ is subject to the system dynamic constraints, where the usual representation is given by a set of Ordinary Differential Equations (ODEs), see Section II, of the form

$$\dot{\mathbf{x}} = f(\mathbf{x}(t), \mathbf{u}(t), t) \quad t \in \Omega \tag{2}$$

The initial and final-time boundary inequality conditions are given by

$$\begin{aligned} B_o(\mathbf{x}(T_o), \mathbf{u}(T_o), T_o) \quad &\leq 0 \\ B_f(\mathbf{x}(T_f), \mathbf{u}(T_f), T_f) \quad &\leq 0 \end{aligned} \tag{3}$$

Conjointly the algebraic trajectory inequality constraints are given by

$$T(\mathbf{x}(t), \mathbf{u}(t), t) \leq 0 \quad t \in \Omega \tag{4}$$

For generality, the boundary and trajectory constraints Eq (3)-Eq (4) have been expressed as inequality constraints, equality constraints can simply be enforced by equating upper and lower bounds. Further, in Eq (1)-Eq (4) the functions $\Phi(.)$, $\Psi(.)$, $f(.)$, $B_i(.)$, and $T(.)$ are assumed to be sufficiently smooth, i.e. at least C^2, and are further defined as follows

$$\begin{aligned} \Phi &: \mathbb{R}^{n_x} \times \mathbb{R}^+ \times \mathbb{R}^{n_x} \times \mathbb{R}^+ \longrightarrow \mathbb{R} \\ \Psi &: \mathbb{R}^{n_x} \times \mathbb{R}^{n_u} \times \mathbb{R}^+ \longrightarrow \mathbb{R} \\ f &: \mathbb{R}^{n_x} \times \mathbb{R}^{n_u} \times \mathbb{R}^+ \longrightarrow \mathbb{R} \\ B_i &: \mathbb{R}^{n_x} \times \mathbb{R}^{n_u} \times \mathbb{R}^+ \longrightarrow \mathbb{R} \\ T &: \mathbb{R}^{n_x} \times \mathbb{R}^{n_u} \times \mathbb{R}^+ \longrightarrow \mathbb{R} \end{aligned} \tag{5}$$

[b] This is generally considered feasible if the TP's computing time is at least a factor 100 smaller than the smallest system time constant.

The solution to the trajectory planning gives the control input, which minimizes the cost functional, while enforcing the constraints

$$\mathbf{u}^*(t) \triangleq \arg \min_{\mathbf{u}(t)\in\mathcal{U}(t,\mathbf{x}(t))} J(\mathbf{x}(t),\mathbf{u}(t),T_o,T_f) \tag{6}$$

IV.A. State And Input Vectors

For our optimal autorotative trajectory, the following thirteen-state and four-input vectors are considered

$$\begin{aligned} \mathbf{x} &= \begin{pmatrix} x_N & x_E & x_Z & \phi & \theta & \psi & u & v & w & p & q & r & \Omega_{MR} \end{pmatrix}^T \\ \mathbf{u} &= \begin{pmatrix} \theta_0 & \theta_{TR} & \theta_{1c} & \theta_{1s} \end{pmatrix}^T \end{aligned} \tag{7}$$

Here, the MR blade collective pitch θ_0 primarily controls vertical helicopter motion and the MR RPM Ω_{MR}; the TR blade collective pitch θ_{TR} primarily controls directional (yaw) helicopter motion; the MR blade lateral cyclic pitch θ_{1c} primarily controls lateral and roll motion; and finally the MR blade longitudinal cyclic pitch θ_{1s} primarily controls longitudinal and pitch motion.

IV.B. Cost Functional

We want to find the optimal autorotative trajectory, corresponding to an initial condition for which a feasible solution exists, i.e. outside the Height-Velocity H-V diagram, see also Section VII.A. Hence, we set the fixed cost such that $\Phi(.) = 0$. Indeed, since the power-off landing trajectory is feasible, the cost $\Phi(.)$ may equivalently be replaced by tight bounds, adjusted for safe landing, on the final values of vehicle kinetic energy and attitude angles. This in turn simplifies the optimization process, and lowers the computational time. Next, the cost functional is defined, from engineering judgment, as a running cost over time such that

$$\begin{aligned} J(\mathbf{x}(t),\mathbf{u}(t),T_o,T_f) \quad &= \int_\Omega \Psi(\mathbf{x}(t),\mathbf{u}(t),t)dt \\ &\int_\Omega \Big[\dot\theta_0^2 + \dot\theta_{1c}^2 + \dot\theta_{1s}^2 + \dot\theta_{TR}^2 \\ &+(\Omega_{MR} - \Omega_{MR_{100\%}})^2 \\ &+u^2 + v^2 + w^2 \\ &+p^2 + q^2 \\ &+(\psi - \psi_f)^2\Big]dt \end{aligned} \tag{8}$$

The term $\dot\theta_0^2 + \dot\theta_{1c}^2 + \dot\theta_{1s}^2 + \dot\theta_{TR}^2$ is added to (i) minimize the battery power consumption, and (ii) encourage smoother control policies, hence avoiding *bang-bang* type solutions, that might excite undesirable high frequency dynamics or resonances.

The term $(\Omega_{MR} - \Omega_{MR_{100\%}})^2$ is added to penalize any large deviations in main rotor speed from its nominal (power on) value. Indeed, a rotor over-speed would increase, beyond acceptable values, the structural stresses on the main rotor hub and hinges, i.e. blade centrifugal stresses. On the other hand, a rotor under-speed would be unsafe for the following two reasons: (i) it increases the region of blade stall, increasing rotor drag and decreasing rotor lift, hence resulting in a higher helicopter sink rate, and (ii) it lowers the stored rotor kinetic energy, which is a crucial element for a good landing flare capability.[77,83]

The term $u^2 + w^2$ is added to limit the excessive build-up of vehicle kinetic energy during the descent. In particular, a high kinetic energy complicates the flare maneuver, since more energy needs to be dissipated, i.e. timing of the controls input becomes increasingly critical.[1]

The term v^2 is added to limit vehicle sideslip flight, as this latter decreases the flight performance, by increasing vehicle drag,[84] and increases the roll/yaw coupling,[85] hence increases the workload of any feedback TT controller.

The term $p^2 + q^2$ is added to maximize the model's linear behavior, by minimizing cross-coupling terms. This is beneficial for the subsequent design of a TT.

Finally, ψ_f refers to the wind heading angle, and the term $(\psi - \psi_f)^2$ is added to encourage flight and landing into the wind. This results in better flight performance, and lowers vehicle kinetic energy at touchdown.

IV.C. Boundary Conditions

The initial boundary conditions $B_o(\mathbf{x}(T_o), \mathbf{u}(T_o), T_o) = 0$ describes the trimmed flight condition $(\mathbf{x}_o, \mathbf{u}_o)$, at the instant just prior to the autorotative maneuver. Further, residual engine power at the instant of failure is neglected in this study. The current analysis focuses only on cases with total loss of power. Now, for the final boundary conditions $B_f(\mathbf{x}(T_f), \mathbf{u}(T_f), T_f) \leq 0$, the aim is here fourfold: (i) set the vehicle on the ground, (ii) account for the vehicle's inherent physical limitations (bounds on main rotor RPM), (iii) provide additional tight bounds on the vehicle kinetic energy and attitude angles, in accordance with technical specifications for safe landing, and (iv) check for the actuators range limitations.

$$\begin{array}{rcl} \mathbf{X}_{lb_f} \leq & \mathbf{x}_f & \leq \mathbf{X}_{ub_f} \\ \mathbf{U}_{lb_f} \leq & \mathbf{u}_f & \leq \mathbf{U}_{ub_f} \end{array} \tag{9}$$

IV.D. Trajectory Constraints

In this paragraph we only review general trajectory constraints, whereas specific obstacle avoidance constraints will be addressed in Section V. For the purpose of general trajectory constraints $T(\mathbf{x}(t), \mathbf{u}(t), t) \leq 0 \quad t \in \Omega$, the aim is here fourfold: (i) account for the vehicle's inherent physical and flight envelope limitations (bounds on speeds, attitude, and main rotor RPM), (ii) account for environmental constraints (the helicopter cannot descend below ground), (iii) check for either the intrinsic actuators dynamic and range limitations or additional control rate limitations[c] set by the designer, and finally (iv) avoid ground strike by the tail rotor blade tip, just before touch-down.

$$\begin{array}{rcl} \mathbf{X}_{lb_t} \leq & \mathbf{x}_f & \leq \mathbf{X}_{ub_t} \\ \mathbf{U}_{lb_t} \leq & \mathbf{u}_f & \leq \mathbf{U}_{ub_t} \\ \dot{\mathbf{U}}_{lb_t} \leq & \dot{\mathbf{u}}_f & \leq \dot{\mathbf{U}}_{ub_t} \\ Z_{lb_t} \leq & x_{Z_{TRBT}} & \leq Z_{ub_t} \end{array} \tag{10}$$

For the Tail Rotor Blade Tip (TRBT) ground clearance, we define the smallest distance between the TRBT and the ground by the distance $x_{Z_{TRBT}}$ in F_I, see figure 2, with the tail rotor radius given by $R_{rot_{TR}}$. Note that both the z-axis of frames F_I and F_b are oriented positive downwards. The F_b position of the tail rotor hub is given by (x_{TR}, y_{TR}, z_{TR}), hence the lowest position of the blade tip, for a positive pitch θ, is given in F_I by

$$x_{Z_{TRBT}} = x_Z + \begin{pmatrix} 0 \\ 0 \\ 1 \end{pmatrix}^T . \mathbb{T}_{Ib} . \begin{pmatrix} x_{TR} - R_{rot_{TR}} . \sin\theta \\ y_{TR} \\ z_{TR} + R_{rot_{TR}} . \cos\theta \end{pmatrix} \tag{11}$$

With the transformation from the body frame F_b to the inertial frame F_I given by

$$\mathbb{T}_{Ib} = \begin{bmatrix} \cos\theta\cos\psi & \sin\theta\sin\phi\cos\psi - \sin\psi\cos\phi & \cos\psi\sin\theta\cos\phi + \sin\phi\sin\psi \\ \sin\psi\cos\theta & \sin\theta\sin\phi\sin\psi + \cos\psi\cos\phi & \sin\theta\cos\phi\sin\psi - \sin\phi\cos\psi \\ -\sin\theta & \cos\theta\sin\phi & \cos\theta\cos\phi \end{bmatrix} \tag{12}$$

Finally, we have $x_{Z_{TRBT}} \leq Z_{safety} < 0$, with Z_{safety} a safety margin.

[c] Additional control input rate constraints may be added to: (i) limit the g factor, hence limiting airframe stress, and (ii) avoid a highly nonlinear behavior, or the so-called *departure susceptibility*, corresponding to the computation of inputs that will excite the nonlinear helicopter dynamics to such an extent as to lead to a loss of stability and/or controllability.[86]

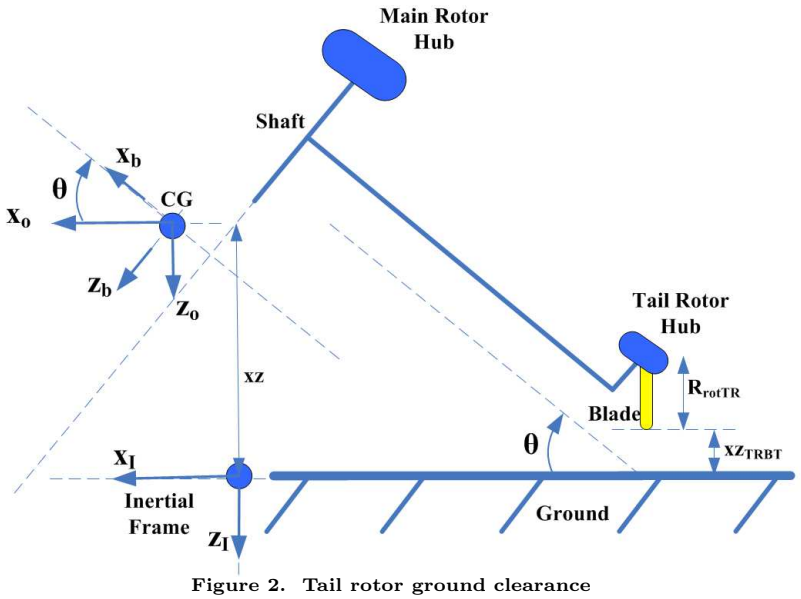

Figure 2. Tail rotor ground clearance

V. Obstacle Avoidance

Trajectory planning with obstacle avoidance is an intrinsically difficult problem to solve, since obstacles generally represent non-convex and non-differentiable polytopic state exclusion regions. Many authors have contributed to the development of obstacle avoidance algorithms, this topic has indeed been a research subject for several decades, hence the literature in this area is extensive, to say the least. An introductory overview, specifically tailored towards UAV trajectory planning, including obstacle avoidance, may be found in Ref. 87, 88. Due to space constraints, we provide here only a very brief overview of earlier work.

Techniques and algorithms to solve the problem of obstacle avoidance may mainly be drawn from research disciplines related to either the artificial intelligence and robotics community, or the (UAV) aerospace-mechanical engineering community. These techniques include: cell decomposition, potential fields, roadmaps and hybrid systems, Mixed Integer Linear Programming (MILP), Receding Horizon Control (RHC), and finally optimal control. In the paradigm of nonlinear optimal control or nonlinear RHC, the obstacle avoidance problem has been addressed through four main avenues: (i) solving a Hamilton-Jacobi-Bellman (HJB) equation, where the set of states that can be steered to a target set, while satisfying bound constraints and avoiding obstacles, is a level set of the value function of the dynamic optimization problem,[89–91] (ii) the addition of a potential function in the objective function, thus converting the collision avoidance problem into an unconstrained optimization,[92] (iii) employing dualization of the state exclusion regions, resulting in maintained continuity of non-differentiable constraints,[93] and (iv) modeling obstacles as differentiable algebraic path constraints, through the use of the continuous-time square-summable sequence space L_p norm,[94] by choosing a sufficiently high value for p.[58, 95]

In this paper, and with the view of using the most straightforward approach, we apply the L_p norm based method, which allows us to create 2-D generic differentiable shapes, such as diamonds, circles, ellipses, squares, rectangles, and their 3-D polyhedron counterparts. In the sequel example, the 3-D obstacle we referred to is a solid cuboid, or convex polyhedron, bounded by six faces. This cuboid can be represented by the following path constraint $O(x, y, z)$, given as

$$O(x,y,z) = \left|\left|\left(\frac{|x-x_c|}{a}, \frac{|y-y_c|}{b}, \frac{|z-z_c|}{c}\right)\right|\right|_p - d \geq 0 \tag{13}$$

With (x_c, y_c, z_c) the 3-D position of the obstacle's center, and the coefficients $\mathbf{C} = (a\ b\ c\ d\ p)^T, \mathbf{C} \in \mathcal{C} \subset \mathbb{R}^5_+$ appropriately chosen. The novel part here consists in defining $\mathbf{C}$ as the solution of a multi-objective, algebraic, nonlinear, constrained optimization problem, given by

$$\mathbf{C}^* \triangleq \arg\min_{\mathbf{C}\in\mathcal{C}} J(\mathbf{C}) \tag{14}$$

Where the multi-objective cost $J(.)$ consists in minimizing $O((x,y,z)_i), i \in \{1,...,6\}$ for each one of the six obstacle faces F_i, with $(x,y,z)_i \in F_i$, hence

$$J(\mathbf{C}) = (||O((x,y,z)_1)||_2 \ ,...,\ ||O((x,y,z)_6)||_2)^T \quad with \quad (x,y,z)_1 \in F_1 \quad ,..., \quad (x,y,z)_6 \in F_6 \tag{15}$$

While having also the constraints

$$\mathbf{C}_{lb} \leq \quad \mathbf{C} \quad \leq \mathbf{C}_{ub} \tag{16}$$

Here, parameter scaling has been applied in order to improve the conditioning of the numerical problem. This optimization can then be solved through standard Sequential Quadratic Programming (SQP) algorithms,[21–23] e.g. with the MATLAB® function *fgoalattain* of the Optimization Toolbox. Then the path constraint $O(x,y,z)$ can be added to the trajectory constraints $T(.)$ of Eq (4).

VI. Direct Optimal Control and The Pseudospectral Discretization

We chose to solve our problem through a direct optimal control method. In this context, the continuous-time optimal control problem is first discretized in some manner and the problem is transcribed to a Non-Linear Programming problem (NLP),[18–20] without formulating an alternate set of optimality conditions as done through indirect methods.[96–99] The resulting NLP can be solved numerically, by well known and efficient optimization techniques, such as Sequential Quadratic Programming (SQP) methods[21–23] or Interior Point (IP) methods.[100–104] These methods in turn attempt to satisfy a set of conditions called the Karush-Kuhn-Tucker (KKT) conditions.[18] Now regarding the discretization of the continuous-time optimal control problem, the three most common discretization approaches to solve an indirect or direct method are: (i) Single-Shooting (SS),[105] (ii) Multiple-Shooting (MS),[106,107] and (iii) State and Control Parameterization (SCP) methods;[108–112] this latter is sometimes also known as transcription in the aerospace community, or as simultaneous strategy in the chemical and process community. Here SS and MS approaches are so-called control parameterization techniques where the control signals alone are discretized,[113] whereas in SCP as indicated by its name, both state and control are parameterized.[114]

Briefly summarized, in shooting techniques the dynamics are satisfied by integrating the differential equations using a time-marching algorithm. The advantage of direct SS is that it generates a small number of variables, while its main disadvantage is that a small change in the initial condition can produce a very large change in the final conditions.[115] Further, the issue of stability is a major concern. Indeed, time integration over a relatively large shooting segment may lead to catastrophic results for unstable systems, and this is why SS generally fails to get a converged solution for such systems.[63] The SS has been most successful in launch vehicle trajectories and orbit transfer problems, primarily because this class of problem lends itself to parameterization with a relatively small number of variables.[116]

On the other hand, direct MS breaks the problem into shorter steps,[115] greatly enhancing the robustness of the shooting method, at the cost of having a larger number of variables. It is then primordial to exploit matrix sparsity to efficiently solve the NLP equations.[116] Despite the increased size of the problem, the direct MS method is an improvement over the standard direct SS method because the sensitivity to errors in the unknown initial conditions is reduced, since the differential equations are integrated over significantly smaller time intervals. Further, MS have shown to be suited for applications of high complexity, having large number of states.[117] However, an additional difficulty exists with the shooting techniques, namely the necessity of defining constrained and unconstrained subarcs a priori, when solving problems with path inequality constraints.[116] This issue however does not exist with SCP methods,[118] which is one of the reasons why SCP methods have actively being investigated.[116]

In addition, SCP methods are known to be very effective and robust,[117] and SCP techniques have been applied to solve nonlinear optimal control problems, such as in space and launch/reentry applications,[109,110,119–123] in aircraft applications,[109,124–127] in helicopter applications,[38,42,43] in UAV applica-

tions,[128–130] and glider applications.[131] Since SCP methods have been intensively researched in the last decade, we present next a general overview of this concept. In SCP, several discretization procedures have been studied, namely local Runge-Kutta methods in Ref. 113, 114, 132, 133, local orthogonal methods in Ref. 108,110,122,134,135, Global Orthogonal Approaches (GOA) or spectral methods in Ref. 16,17,135–140, and most recently hybrid local/global methods in Ref. 141. Of these four procedures, the GOA have received much attention in the last decade, since they have the advantage of providing spectral convergence, i.e. at an exponential rate, for the approximation of analytic, i.e. sufficiently smooth, functions.[142–144] Thus, for a given error bound, GOA methods generate a significantly smaller scale optimization problem when compared to other methods.[143] This is an important aspect since the efficiency and even convergence of NLPs improves for a problem of smaller size.[145]

In a GOA the system's state-vector is expressed as a truncated series expansion, characterized by BAsis (BA) functions, and Expansion Coefficients (EC) determined from test functions, which attempt to ensure that the Ordinary Differential Equations (ODEs), defining the system dynamics, are optimally satisfied. The choice of the BA functions is what distinguishes GOA methods from finite-difference or finite-element methods. In both finite-type methods, the BA is local in character, while for GOA methods the BA consists of infinitely differentiable global functions, such as orthogonal polynomials,[146] trigonometric functions, or constant basis function like Haar[147] or block-pulse. Further, the EC distinguish the three most common types of GOA methods, namely Galerkin, Tau, and collocation. Of these three, the last one, often referred to as the PseudoSpectral (PS) discretization, has received considerable attention in recent years. In PS methods, the BA is described by Lagrange interpolating polynomials,[148] and are expressed using a set of N support points. The location of these support points is determined by orthogonal polynomials, for example Legendre polynomials,[146] although other choices exist, such as Chebyshev polynomials.[149] Besides the choice of these N support points, another set of K points is required for the discretization of the integral within the cost functional, and the system dynamic constraints. These K points are chosen such that the quadrature approximation of an integral is minimized.[148] Now, it is well known that the highest accuracy quadrature approximation, for a given number of K points, is the Gauss quadrature.[148] In this case, the location of these K quadrature points, called Legendre-Gauss (LG) points, is determined by the roots of a Kth-degree Legendre polynomial.[16,17] It is also worth noting that two additional variations to the LG approach have extensively been investigated in the last decade, namely the Legendre-Gauss-Lobatto (LGL) method,[136,137] and the Legendre-Gauss-Radau (LGR) method.[135,139,140] It was further reported in Ref. 150 that the LG and LGR methods have been found to be very similar in accuracy, while outperforming the LGL method.

PS methods have been extensively used in solving fluid dynamics problems,[14,15] but only recently have these methods been used for solving a variety of optimal control problems. It is clear that PS methods exhibit a number of advantages when compared to other discretization methods, even when compared to the popular spline parametrization.[115,128,151] Indeed, PS techniques have been widely used in space and launch/reentry applications, see the results of Ref. 152–169. However, they have so far only seen limited use in other aeronautical applications such as: aircrafts,[157,170–173] helicopters,[174] fixed-wing UAVs,[58,159,175–177] and helicopter UAVs.[65,178] Accordingly, we opt for a PS numerical structure, as the discretization framework for our trajectory generation problem.

VII. Simulation Results

Our simulation software uses the helicopter UAV flight dynamics model presented in Section II, also referred in table 2, and implemented in a MATLAB® environment. To solve the nonlinear control problem, the pseudospectral numerical method, as described in Section VI, is used. This numerical discretization framework is available in a MATLAB environment, through the open-source General Pseudospectral OPtimal control Software GPOPS®.[138,179–181] In order to use GPOPS, the optimal control problem must first be reformulated into a GPOPS format, as a set of MATLAB m-files.[181] Second, the helicopter model must also be expressed in a vectorized structure, implying that each model variable and parameter is a vector, which values are time-dependent. This latter aspect is particularly relevant for complex models, where for instance standard matrix-matrix multiplications have to be handled with care, as each matrix element is a vector. Third, (cubic) B-Splines interpolating functions ought to be used, when querying lookup tables, as the spectral convergence of PS methods only holds when the functions under consideration are smooth.[146,182]

Finally, it is best practice to non-dimensionalize and scale model variables and quantities, in order to improve conditioning of the numerical problem. Once the control problem has been discretized, it is then transcribed into a static, finite-dimensional NLP optimization problem. An NLP is generally sparse, and many well-known efficient optimization techniques exist to numerically solve large-scale and sparse NLPs. In our case, we use the SNOPT® software,[23] which solves finite-dimensional optimization problems through SQP. In the sequel, the discretization of the optimal autorotative flight problem uses 33 nodes, yielding a NLP problem having 691 variables and 578 constraints. Further, finite differencing has been used to estimate the objective gradient and constraint Jacobian. In this case, the computational time for a single trajectory, on a legacy computer hardware, is in the range of one to two hours.

	Definition	Parameter	Value	Unit
Vehicle	Total mass	m_{Zerof}	8.35	kg
	Inertia moment wrt x_b	A	0.338	$kg.m^2$
	Inertia moment wrt y_b	B	1.052	$kg.m^2$
	Inertia moment wrt z_b	C	1.268	$kg.m^2$
	Inertia product wrt x_b	D	0.001	$kg.m^2$
	Inertia product wrt y_b	E	0.002	$kg.m^2$
	Inertia product wrt z_b	F	0	$kg.m^2$
Main Rotor	Direction of rotation	Γ	-1 (CW)	
	Number of blades	N_b	2	
	Nominal angular velocity	$\Omega_{MR_{100\%}}$	151.84	rad/s
	Rotor radius from hub	R_{rot}	0.933	m
	Blade mass	M_{bl}	0.218	kg
Tail Rotor	Number of blades	$N_{b_{TR}}$	2	
	Nominal angular velocity	$\Omega_{TR_{100\%}}$	709.11	rad/s
	Rotor radius from hub	$R_{rot_{TR}}$	0.17	m

Table 2. Helicopter configuration

We present next simulation results for a limited number of initial trimmed flight conditions, in a zero-wind environment. But first we review the Height-Velocity (H-V) diagram.

VII.A. The Height-Velocity Diagram

For certain combinations of altitude Above Ground Level (AGL) and airspeed, the capability of a helicopter to perform a safe autorotative landing is limited by the structural and aerodynamic design of the helicopter.[183] In fact, power failure within the dangerous or unsafe regions, defined by these combinations of AGL and airspeed, may result in high risk of severe damage or loss of vehicle. These limiting combinations of AGL and airspeed are often expressed as the H-V diagram[d]. Knowledge of these dangerous regions is important for safety procedures and operational reasons. Ideally, one would like to eliminate these unsafe regions altogether, or at least reduce their size. H-V investigations can be traced back to the late 1950s and early 1960s.[184–186] For example, eliminating the H-V restrictions was demonstrated with the *Kolibrie* helicopter, built by the *Nederlandse Helikopter Industrie (NHI)* in the late 1950s. It was designed by Dutch helicopter engineers and pioneers Jan M. Drees and Gerard F. Verhage. The helicopter was ram-jet powered, with these latter being positioned at the blade tips. This resulted in very high main rotor rotational inertia. The H-V subject was also investigated in Ref. 183, where flight-test data was used to derive semi-empirical functions of a generalized non dimensional H-V diagram, independent of density altitude and gross weight variations. In Ref. 187 it was pointed out that high rotor inertia, low disk loading, and a high maximum thrust coefficient could reduce the size of the unsafe zone. In Ref. 188, 189, the concept of the so-called High Energy Rotor (HER) was studied, using blades with high rotational inertia. The goal of the HER was to eliminate the unsafe regions, but also to allow for less demanding autorotation maneuvers, and finally use the rotor kinetic energy as a source of transient power for better maneuverability. Additional results can also be found in Ref. 190, 191 where recent flight tests, related to the H-V subject with the Bell 430 and 407

[d] Also called the *deadmans* zone

helicopters, have been presented.

We compute for our UAV the corresponding H-V diagram, based upon specific flight envelope and control input boundaries, with these latter being given in table 3. For a bounded state-vector final value, in accordance with technical specifications for safe landing, the H-V diagram is the solution of an optimization problem, similar to the general one presented in Section IV. Either a minimization/maximization of altitude problem is solved, or a feasibility problem is tested. In this latter case, the cost objective $J(.)$ of Eq (1) is set to zero, and one only requires to check whether safe landing is feasible, for a range of initial conditions. The minimization/maximization approach often led the solver to run into numerical difficulties. These difficulties were caused by: (i) the inclusion of highly nonlinear lookup tables which, even though cubic B-Splines interpolation has been used, have shown to have a detrimental effect on problem smoothness, and (ii) the possible existence of a large number of solutions that all yield approximately the same value of the cost objective, in other words, the objective index is rather insensitive to the solution trajectory in the neighborhood of the optimal solution.[124] These two aspects will briefly be addressed in Section VIII. Hence, we opted here for the simpler feasibility approach.

	Definition	Parameter	Range	Unit
Flight Envelope	Roll angle	ϕ	[-48,48].π/180	rad
	Pitch angle	θ	[-48,48].π/180	rad
	Yaw angle	ψ	[0,360].π/180	rad
	Body longitudinal velocity	u	[-5,20]	m/s
	Body lateral velocity	v	[-5,5]	m/s
	Body vertical velocity	w	[-5,20]	m/s
	Body roll angular velocity	p	[-200,200].π/180	rad/s
	Body pitch angular velocity	q	[-200,200].π/180	rad/s
	Body yaw angular velocity	r	[-400,400].π/180	rad/s
	Main rotor RPM ($\Omega_{MR_{100\%}}$ = 1450 RPM)	Ω_{MR}	[70% .$\Omega_{MR_{100\%}}$, ... ,110% .$\Omega_{MR_{100\%}}$].2π/60	rad/s
Actuators	MR collective	θ_0	[-2.8,13.7].π/180	rad
	TR collective	θ_{TR}	[-27,32.8].π/180	rad
	MR lateral cyclic	θ_{1c}	[-6.8,6].π/180	rad
	MR longitudinal cyclic	θ_{1s}	[-7.8,5].π/180	rad
	MR collective rate	$\dot{\theta}_0$	[-52,52].π/180	rad/s
	TR collective rate	$\dot{\theta}_{TR}$	[-120,120].π/180	rad/s
	MR lateral cyclic rate	$\dot{\theta}_{1c}$	[-56,56].π/180	rad/s
	MR longitudinal cyclic rate	$\dot{\theta}_{1s}$	[-56,56].π/180	rad/s

Table 3. Flight envelope and control input boundaries

The results are shown in figure 7, for a coarse grid, with steps of 1 m in AGL and 1 m/s in airspeed. Our UAV exhibits only a low-speed unsafe zone. We further subdivide this unsafe zone into a high-risk zone, shown in red (for which the number of violated constraints is above a certain threshold), and a medium-risk zone shown in magenta.

VII.B. Optimal Autorotation

To start, we consider initial conditions at hover, for three different AGL, see table 4, in a Southbound path. First, figure 3 and figure 4 show the input control rate activity, where the magenta horizontal lines display hard bounds on variables. For all test cases, we see that the vertical (MR collective) and longitudinal channels display the highest level of activity. This is to be expected, since (i) the heading goal $\psi_f = 180°$ is identical to the initial one, (ii) the lateral velocity v^2 is minimized, (iii) the East position of the landing site is not restricted to any particular location, and (iv) the test cases do not include any (side-)wind effects; hence solicitation of lateral control is minimal. This is translated in the minimal activity of lateral cyclic

and tail rotor collective controls of figure 5 and figure 6, where we also note the gradual control movements, in accordance with control rate minimization.

Test Case	Airspeed (m/s)	Altitude (AGL) (m)	Line Color in Figures
$C1$	hover	25	Red (solid line)
$C2$	hover	40	Blue (dotted line)
$C3$	hover	110	Black (dashed line)

Table 4. Initial conditions: variation of altitude

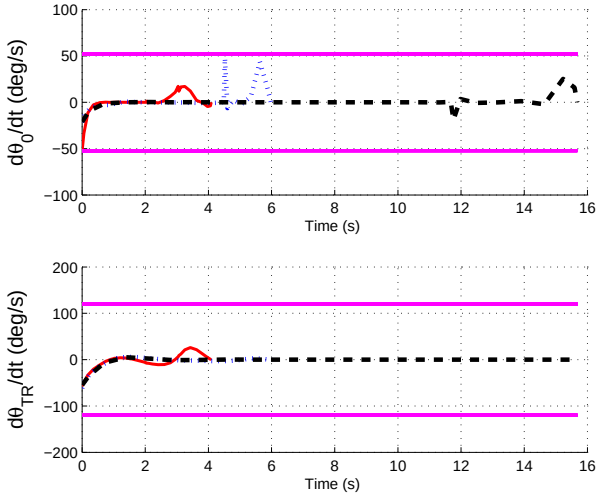

Figure 3. MR & TR collective control input rates, starting in hover

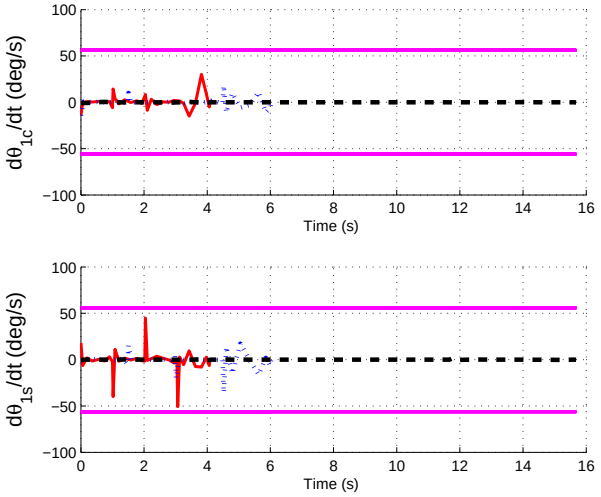

Figure 4. MR Lat./Long. cyclic control input rates, starting in hover

Further in figure 5, we see the collective going full-down, as soon as the maneuver initiates. As expected, this is necessary in order to minimize main rotor RPM decay, see figure 8. Besides, collective also sharply increases as the helicopter nears to the ground, to prevent rotor over-speed, while reducing the sink rate. In addition, longitudinal cyclic is used to (i) manage vehicle and main rotor kinetic energies, (ii) reduce forward airspeed, and (iii) level the attitude for a proper landing. This can be checked in figure 9, where, for low AGL initial conditions, we see the vehicle pitch-up and pitch-down during flare. Also, for low AGL initial conditions, figure 9 and figure 10 show the limited displacements on the yaw, and lateral velocity channels, consistent with the anticipated behavior.

In addition, figure. 11 presents the trajectory inertial position in 3-D. Again, lateral displacement is minimal. We note that, for hover initial conditions, the optimal autorotative trajectory starts to resemble a pure vertical flight path, as the AGL increases, which confirms the results of Ref. 30.

Next, we consider initial conditions at an AGL of 40 m, for three different airspeeds, see table 5, in again a Southbound path. Now, due to space constraints, we only discuss the salient features of these three $C4, C5, C6$ cases, without reviewing all figures in detail. From figure 14, figure 15 and figure 16, we note that despite big differences in initial kinetic energy, the flight time, rate of descent, and flare maneuver are very similar, whereas the traveled distance does increase as a function of initial energy. In addition we see that if differences, between the hover/low-speed cases $C4, C5$ and the high speed case $C6$, are to be noted, then they tend to mainly appear on the longitudinal and RPM channels, during the initial flight phase, see figure 12, figure 13, and figure 14. Finally, we also computed the optimal flight paths in case of tail rotor failure, and for the case of landing site constraints (e.g. a turn-back maneuver for a landing on the departure runway). However, these cases will not be discussed here due to space constraints.

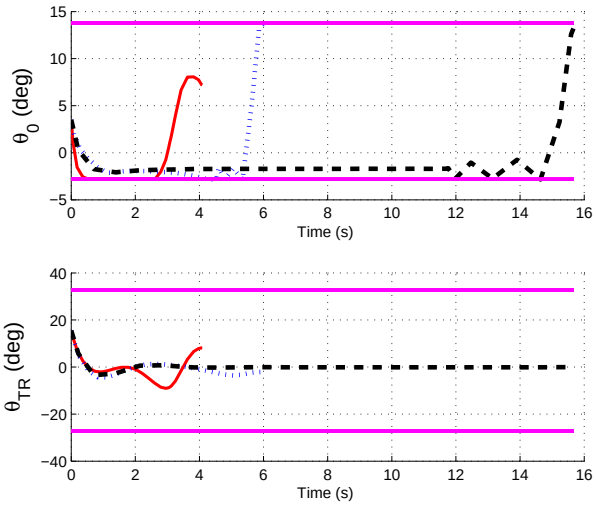

Figure 5. MR & TR collective control inputs, starting in hover

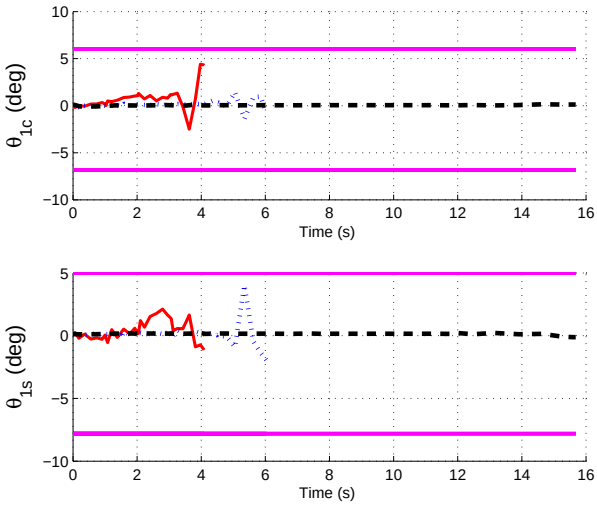

Figure 6. MR Lat./Long. cyclic control inputs, starting in hover

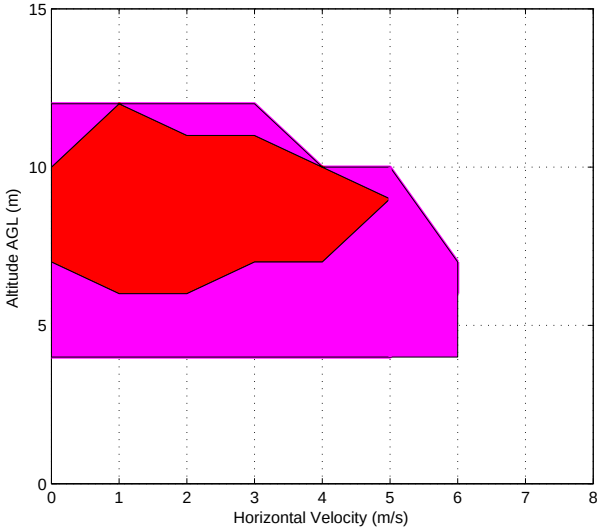

Figure 7. Height-Velocity (H-V) diagram

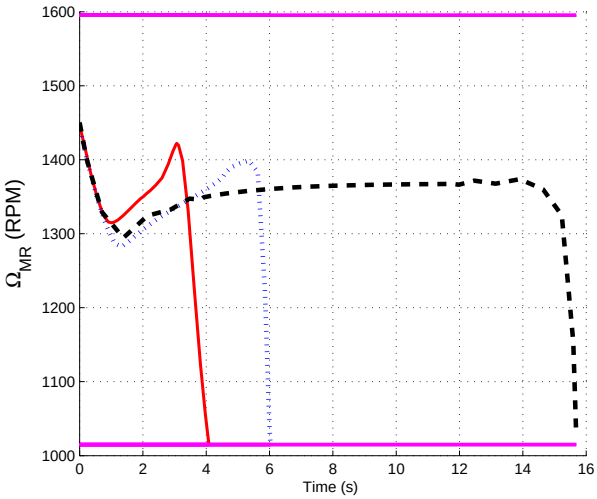

Figure 8. Main Rotor RPM, starting in hover

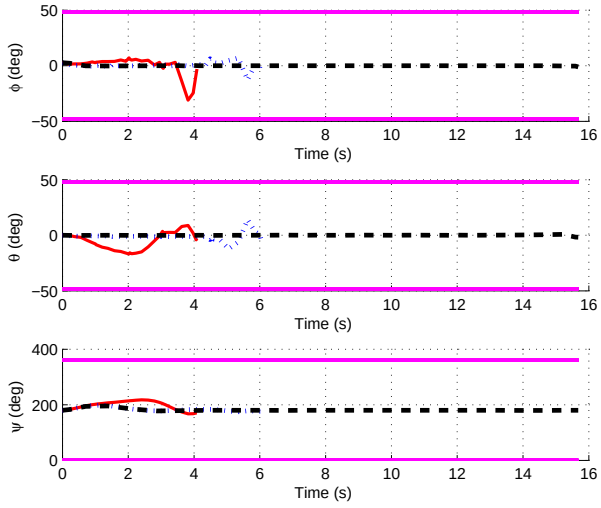

Figure 9. Euler angles, starting in hover

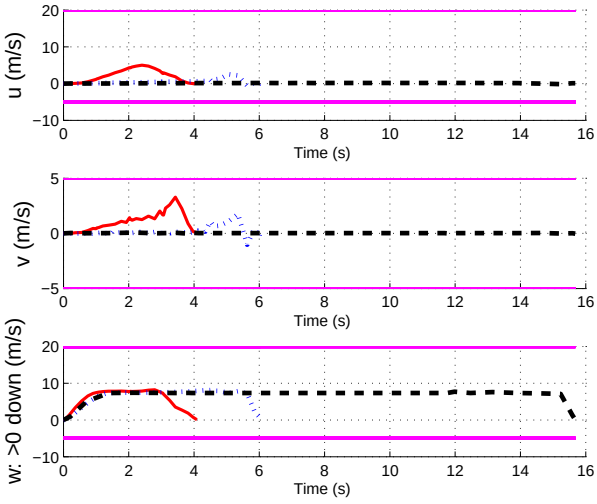

Figure 10. Body linear velocities, starting in hover

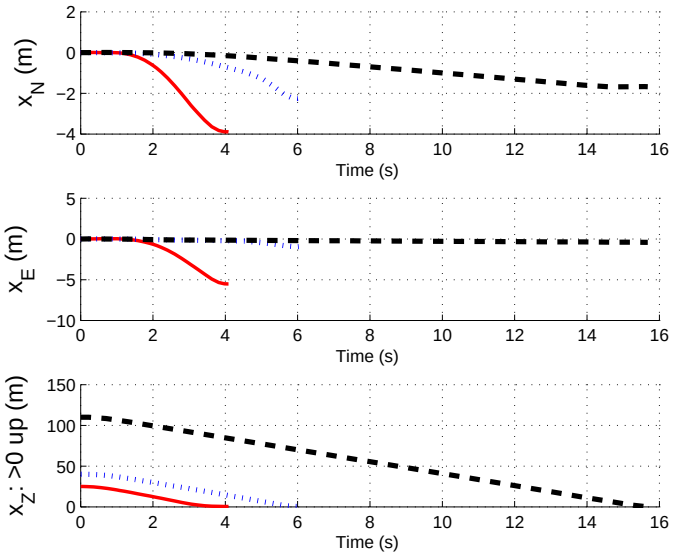

Figure 11. Inertial position (NEU), starting in hover

Test Case	Airspeed (m/s)	Altitude (AGL) (m)	Line Color in Figures
$C4$	hover	40	Red (solid line)
$C5$	5	40	Blue (dotted line)
$C6$	15	40	Black (dashed line)

Table 5. Initial conditions: variation of airspeed

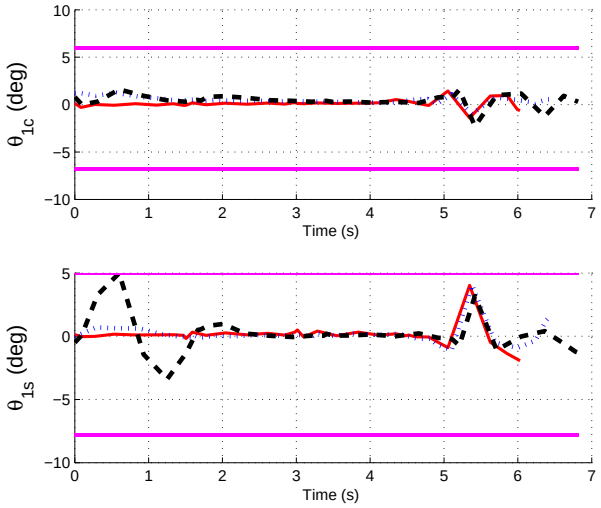

Figure 12. MR Lat./Long. cyclic control inputs, starting at 40 m AGL

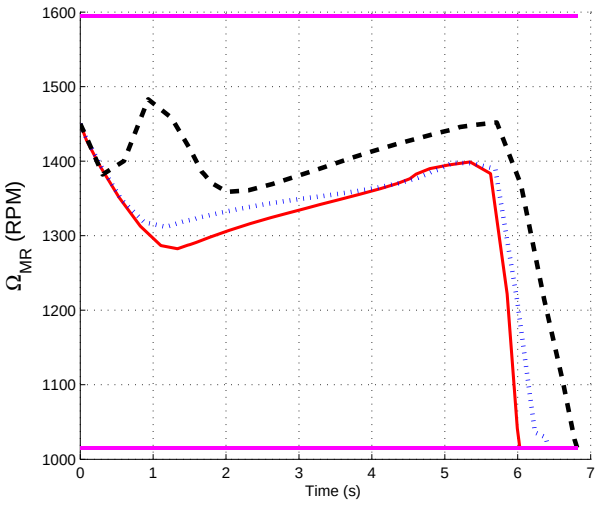

Figure 13. Main Rotor RPM, starting at 40 m AGL

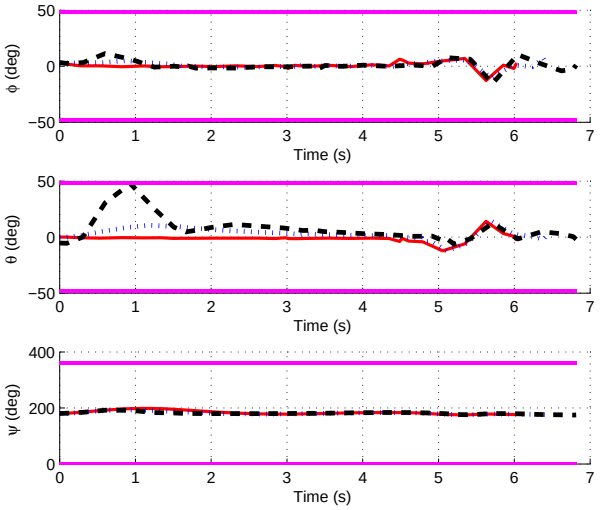

Figure 14. Euler angles, starting at 40 m AGL

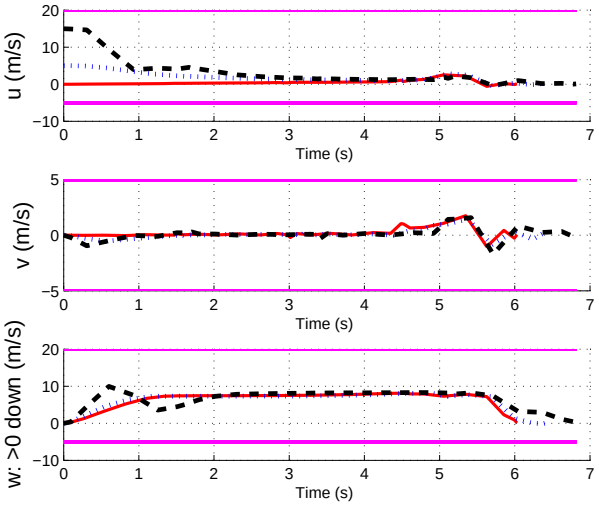

Figure 15. Body linear velocities, starting at 40 m AGL

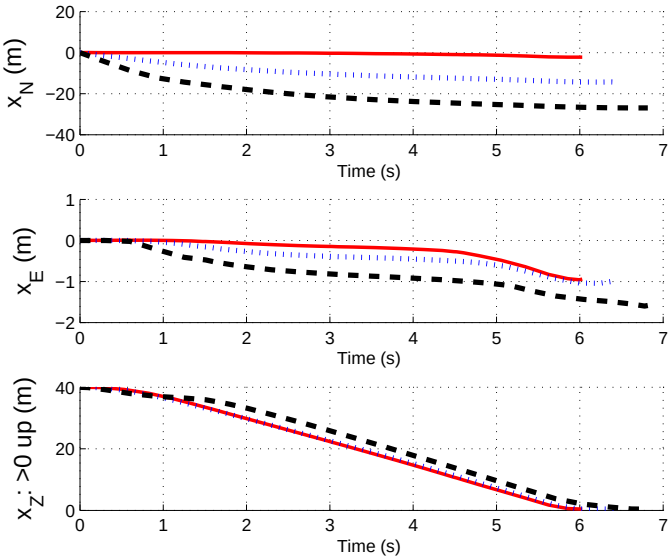

Figure 16. Inertial position (NEU), starting at 40 m AGL

VII.C. Optimal Autorotation with Obstacle Avoidance

We demonstrate here the obstacle avoidance functionality. A building of following dimensions $(-50, -35)m$ on the North/South axis, $(-10, 10)m$ on the East/West axis, and $(-40, 0)m$ on the vertical axis, has been modeled with the method outlined in Section V. For this obstacle we have $(x_c, y_c, z_c) = (-42.5, 0, -20)$ and we obtain $(a, b, c, d, p) = (50.6, 63.9, 111.6, 0.18, 50)$. The initial start condition is at an AGL of 50 m, with an airspeed of 15 m/s, in a Southbound path. The first simulation, in figure 17, shows the optimal autorotative flight path while ignoring the presence of the obstacle, whereas the second simulation, shown in figure 18, gives the optimal flight path which also avoids the obstacle.

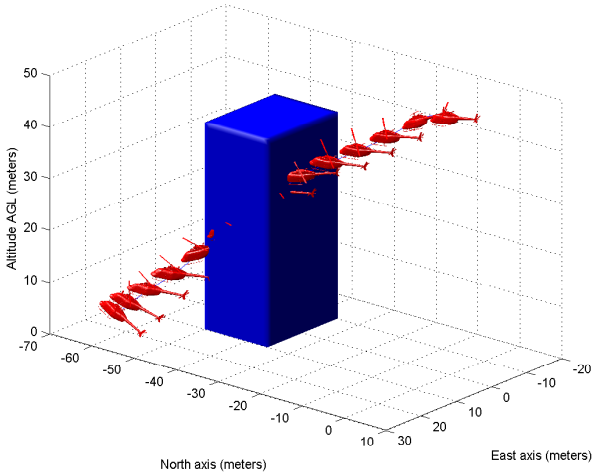

Figure 17. Optimal trajectory, while ignoring the presence of the obstacle

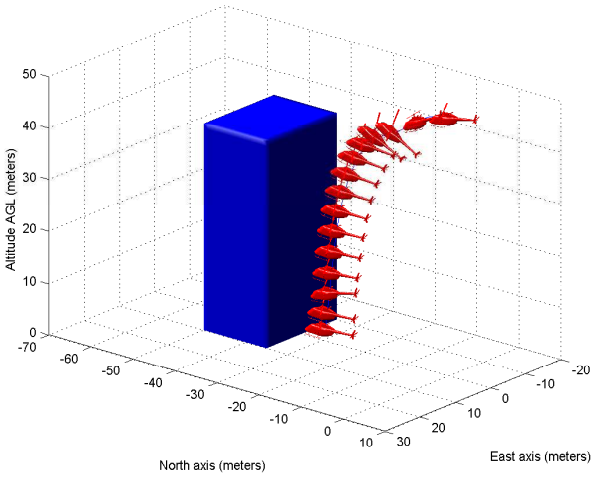

Figure 18. Optimal trajectory, while avoiding the obstacle

VIII. Discussion

As stated earlier in Section VI, direct optimal control methods have several advantages. Specifically, the first-order necessary conditions do not need to be explicitly derived, and the large radii of convergence allow for less accurate initial guess on states and control inputs. Hence, direct methods are appealing for complicated applications.[116] Further, pseudospectral (PS) methods have the known advantage of providing exponential rate convergence for the approximation of analytic functions.[143,144,146,182] For all that, the direct optimal method used in our application has also shown some inherent limitations.

First, it is in some cases uncertain whether the solution obtained is truly optimal.[17] Indeed, it is well known that a solution may show sensitivity to the type of discretization scheme, and time integration used.[51,192] For example, fluctuated solutions have been seen as the number of discretization nodes was varied. Second, we noticed that the use of aerodynamic coefficients lookup tables has had a negative impact on the exponential convergence, even when queried with cubic B-Splines interpolating functions. This effect gets exacerbated for highly nonlinear tabulated data, such as fuselage aerodynamic coefficients variations as a function of sideslip angle. Here, solving the optimal control problem may become at times computationally intractable, and at times either unfeasible or feasible, but sub-optimal. Note that nonsmooth solutions, or nonsmooth problem formulations, are far from uncommon in the aerospace domain. In fact, to mitigate this known issue, several approaches have been investigated, such as: (i) a PS knotting method in Ref. 182, (ii) a hybrid global/local collocation method in Ref. 141, and (iii) additional results in Ref. 134, 193, 194. For our optimal problem, implementing one of these approaches may be seen as a topic for future research. Third, the resulting NLP is numerically solved through a SQP method. SQP belong to the clas of iterative, gradient-based methods. The basic principle is to replace the given nonlinear problem by a sequence of quadratic subproblems that are easier to solve. Beforehand, an initial guess of the unknown decision vector is required, and then for each iteration, a search direction and corresponding step length are computed, and further used to provide a new value of this decision vector.[144] Gradient methods are known as local methods, hence upon convergence, a local optimum will generally be obtained. Indeed, and although direct

methods have large radii of convergence, we did notice this sensitivity to local minima, by obtaining distinct optimal solutions, for distinct initial guesses. To mitigate this problem, a classical iterative approach for initial guess refinement may be used.[51] The idea is to first compute a cheap optimal solution, using very few discretization nodes. Then use this solution as the initial guess to an optimal control problem, having this time a slightly higher number of nodes. This iterative scheme is repeated until a solution, with the desired number of nodes, is reached. Fourth, the final time T_{f_o} of an optimal trajectory is defined over the time domain $\Omega = (T_o, T_f)$. For the sake of problem feasibility, T_f needs to be chosen sufficiently high, hence we have $T_{f_o} \leq T_{f_{min}} \leq T_f$ with $T_{f_{min}}$ defined as

$$T_{f_{min}} \triangleq \min\{T_f | T_{f_o} \leq T_f \quad \forall (T_f, T_{f_o}) \in \mathbb{R}^2_+\} \tag{17}$$

We have observed that the optimal trajectories were sensitive to increases in T_f, even though the T_f values were nonbinding constraints. This is a result from the nonconvexity of our problem. This property of solution jumps, for nonconvex problems, when nonbinding constraints are either added, modified, or removed is a well-known phenomenon in optimization.[20] Hence, if optimal trajectories need to be evaluated against each-other, it would probably be best practice to include the final time T_f in the fixed cost $\Phi(.)$.[124] Finally, one should remember that the obtained solution provides only the state and control values at the discrete nodes, since in our case we did not use any mesh refinement grid in order to keep the problem computationally tractable. The optimal solution satisfies only the discretized constraints, and is said to be discrete-time feasible.[162] Consequently, obtaining a valid solution to the original continuous-time problem requires a mapping of the discrete solution to the continuous-time domain, which is usually achieved through some kind of interpolation. However, after such a mapping, the discrete-time feasible solution may not be feasible to the continuous-time problem.[162] This is due to the introduction of approximation errors, as a result of the discretization and interpolation. One obvious way to mitigate this problem is to increase the number of discretization nodes, although using Bellman's principle of optimality may also be considered.[165, 195]

IX. Conclusion

We derive optimal power-off, or autorotative, landing trajectories, for the case of a small-scale helicopter UAV. These open-loop optimal trajectories, generated by a Trajectory Planner (TP), represent the solution to the minimization of a cost objective, given system dynamics, controls and states equality and inequality constraints. Our cost objective maximizes flight performance and control smoothness, while minimizing roll-yaw coupling, hence lowering the workload of any feedback Trajectory Tracker (TT) controller. Height-Velocity diagram computation, and further obstacle avoidance and energetic parsimony of the trajectories produced by the planner were also demonstrated in simulations. Hence, for a range of initial conditions, optimal autorotative trajectories can be computed off-line by a TP, and stored as lookup tables, on-board a flight control computer. By so doing, these trajectories provide both the optimal states to be tracked by a feedback trajectory tracker, and the feedforward nominal controls needed to track the trajectory.

In this case, it would particularly be interesting to analyze the robustness of the obtained trajectories, with respect to model uncertainties, i.e. unmodeled higher-order dynamics, unmodeled static nonlinearities, and parametric uncertainties. Although results on static robust optimization have been proven, the field of (dynamic) robust optimization, for high-order systems, is still in its infancy. Another extension concerns the robustness of the obtained trajectories, with respect to signal uncertainties, i.e. wind disturbances and signal noise; problems at the heart of stochastic optimization. Finally, each new helicopter configuration, modifying main rotor inertia or vehicle weight, may likely result in distinct optimal solutions. In order to limit the on-board memory requirement, resulting from the storage of a large family of optimal reference trajectories, it would be beneficial to express these optimal solutions in a non-dimensional form, thus independent of specific helicopter configurations. These aspects, together with the design of the trajectory tracker controller, have been identified as topics for future research.

References

[1]Taamallah, S., "A Qualitative Introduction to the Vortex-Ring-State, Autorotation, and Optimal Autorotation," *Europ. Rotorcraft Forum*, 2010.

[2]Bachelder, E. N. and Aponso, B. L., "An Autorotation Flight Director for Helicopter Training," *Am. Helicopter Soc.*, 2003.

[3]Aponso, B. L., Bachelder, E. N., and Lee, D., "Automated Autorotation for Unmanned Rotorcraft Recovery," *AHS Int. Specialists' Meeting On Unmanned Rotorcraft*, 2005.

[4]Aponso, B. L., Lee, D., and Bachelder, E. N., "Evaluation of a Rotorcraft Autorotation Training Display on a Commercial Flight Training Device," *J. of the Am. Helicopter Soc.*, 2007.

[5]Hart, S., "Analysis of Civil Helicopter Accidents," *Proceedings of the HeliExpo '98*, 1998.

[6]Pleasants, W. A. and White, G. T., "Status of Improved Autorotative Landing Research," *Army Science Conf., West Point*, 1980.

[7]Rogers, S. P. and Asbury, C. N., "A Flight Training Simulator for Instructing the Helicopter Autorotation Maneuver (Enhanced Version)," Tech. Rep. TR FR-1372, NASA AMES, 2000.

[8]McIntyre, H. H., "A Simplified Study of High Speed Autorotation Entry Characteristics," *Am. Helicopter Soc.*, 1970.

[9]Aponso, B. L., Lee, D., and Bachelder, E. N., "Evaluation of a Rotorcraft Autorotation Training Display on a Commercial Flight Training Device," *Am. Helicopter Soc.*, 2005.

[10]Keller, J. D., McKillip, R. M., Horn, J. F., and Yomchinda, T., "Active Flight Control and Applique Inceptor Concepts for Autorotation Performance Enhancement," *Am. Helicopter Soc.*, 2011.

[11]Harris, F. D. and Scully, M. P., "Helicopters Cost Too Much," *Am. Helicopter Soc.*, 1997.

[12]Selier, M., Taamallah, S., Smit, E. J., and Haverdings, H., "NLR Activities on Small Autonomous Helicopters. Intermediate Results and Lessons Learnt Under the NIVR Basic Research Programme," Tech. Rep. NLR-CR-2005-680, NLR, 2005.

[13]Taamallah, S., Bombois, X., and Van den Hof, P. M. J., "Optimal Control For Power-Off Landing Of A Small-Scale Helicopter A Pseudospectral Approach," *Am. Control Conf.*, 2012.

[14]Gottlieb, D., Hussaini, M. Y., and Orszag, S. A., "Theory and Applications of Spectral Methods," *SpectralMethods for PDEs. Soc. of Industrial and Applied Mathematics (SIAM)*, 1984.

[15]Canuto, C., Hussaini, M. Y., Quarteroni, A., and Zang, T. A., *Spectral Methods in Fluid Dynamics*, Springer-Verlag, New York, 1988.

[16]Benson, D. A., *A Gauss Pseudospectral Transcription for Optimal Control*, Ph.D. thesis, Massachusetts Institute of Technology, 2004.

[17]Huntington, G. T., *Advancement and Analysis of a Gauss Pseudospectral Transcription for Optimal Control*, Ph.D. thesis, Massachusetts Institute of Technology, 2007.

[18]Bertsekas, D., *Nonlinear Programming - Second Edition*, Athena Scientific, Belmont, MA, 1999.

[19]Nocedal, J. and Wright, S., *Numerical Optimization*, Springer, NY, 2000.

[20]Bazaraa, M. S., Sherali, H. D., and Shetty, C. M., *Nonlinear Programming: Theory and Algorithms - Third Edition*, Wiley-Interscience, 2006.

[21]Gill, P. E., Murray, W., and Saunders, M. A., "SNOPT: An SQP Algorithm for Large-Scale Constrained Optimization," *SIAM Reviews*, Vol. 47, 2002, pp. 99–131.

[22]Gill, P. E., Murray, W., Saunders, M. A., and Wright, M. H., "Users Guide for SNOPT Version 7: Software for Large-Scale Nonlinear Programming," Tech. rep., University of California San Diego, 2008.

[23]SBS-Inc., http://www.sbsi-sol-optimize.com/asp/sol_product_snopt.htm, Stanford University, U.S.A.

[24]Schaal, S., *Learning from Demonstration (in Advances in Neural Information Processing Systems)*, Edited by M. C. Mozer, M. I. Jordan, and T. Petsche (MIT Press), Cambridge, 1997.

[25]Abbeel, P., Coates, A., Quigley, M., and Ng, A. Y., "An application of reinforcement learning to aerobatic helicopter flight," *NIPS 19*, 2007.

[26]Abbeel, P., Coates, A., Hunter, T., and Ng, A. Y., "Autonomous Autorotation of an RC Helicopter," *11th Int. Symposium on Experimental Robotics (ISER)*, 2008.

[27]Lee, D. J., Bang, H., and Baek, K., "Autorotation of an Unmanned Helicopter by a Reinforcement Learning Algorithm," *AIAA Guidance, Navigation and Control Conf.*, 2008.

[28]Uemura, M., Ishikawa, M., Sudo, N., Sudo, I., and kubo, Y., "Fuzzy Intelligent Pilot Support System for an Autorotative Flight of Helicopter," *Europ. Rotorcraft Forum*, 1993.

[29]Komoda, M., "Prediction of Height-Velocity Boundaries for Rotorcraft by Application of Optimizing Techniques," *Trans. of the Japan Soc. for Aeronautical and Space Sciences*, Vol. 15, No. 30, 1973, pp. 208–228.

[30]Johnson, W., "Helicopter Optimal Descent and Landing After Power Loss," Tech. Rep. TM 73-244, NASA Ames Research Center, 1977.

[31]Lee, A. Y., Bryson, A. E., and Hindson, W. S., "Optimal Landing of a Helicopter in Autorotation," *AIAA J. of Guidance, Control, and Dynamics*, Vol. 11, No. 1, 1988, pp. 7–12.

[32]Okuno, Y., Kawachi, K., Azuma, A., and Saito, S., "Analytical Prediction of Height-Velocity Diagram of a Helicopter Using Optimal Control Theory," *AIAA J. of Guidance, Control, and Dynamics*, Vol. 14, No. 2, 1991, pp. 453–459.

[33]Okuno, Y. and Kawachi, K., "Optimal Control of Helicopters Following Power Failure," *AIAA J. of Guidance, Control, and Dynamics*, Vol. 17, No. 1, 1994, pp. 181–186.

[34]Floros, M. W., "DESCENT Analysis for Rotorcraft Survivability with Power Loss," *Am. Helicopter Soc.*, 2009.

[35]Lee, A., "Engineering Notes - Optimal Autorotational Descent of a Helicopter with Control and State Inequality Constraints," *AIAA J. of Guidance, Control, and Dynamics*, Vol. 13, No. 5, 1990, pp. 922–924.

[36]Jhemi, A. A., Carlson, E. B., Zhao, Y. J., and Chen, R. T. N., "Optimization of Rotorcraft Flight Following Engine Failure," *J. of the Am. Helicopter Soc.*, 2004.

[37]Bottasso, C. L., Croce, A., Leonello, D., and Riviello, L., "Optimization of Critical Trajectories for Rotorcraft Vehicles," *J. of the Am. Helicopter Soc.*, 2005, pp. 165–177.

[38]Bottasso, C. L., Chang, C. S., Croce, A., Leonello, D., and Riviello, L., "Adaptive Planning and Tracking of Trajectories for the Simulation of Maneuvers with Multibody Models," *Computer Methods in Applied Mechanics and Engineering*, 2006.

[39]Carlson, E. B., Xue, S., Keane, J., and Burns, K., "H-1 Upgrades Height-Velocity Diagram Development Through Flight Test and Trajectory Optimization," *Am. Helicopter Soc.*, 2006.

[40]Bibik, P. and Narkiewicz, J., "Helicopter Modeling and Optimal Control in Autorotation," *Am. Helicopter Soc.*, 2008.

[41]Bibik, P. and Narkiewicz, J., "Helicopter Optimal Control in OEI Low Speed Flights," *Europ. Rotorcraft Forum*, 2008.

[42]Bottasso, C. L., Maisano, G., and Luraghi, F., "Efficient Rotorcraft Trajectory Optimization Using Comprehensive Vehicle Models by Improved Shooting Methods," *Europ. Rotorcraft Forum*, 2009.

[43]Bottasso, C. L., Maisano, G., and Scorcelletti, F., "Trajectory Optimization Procedures for Rotorcraft Vehicles, Their Software Implementation, and Applicability to Models of Increasing Complexity," *J. of the Am. Helicopter Soc.*, 2010.

[44]Floros, M. W., "Application of Sequential Quadratic Programming to Rotorcraft Survivability with Power Loss," *Am. Helicopter Soc.*, 2011.

[45]Dalamagkidis, K., Valavanis, K. P., and Piegl, L. A., "Autonomous Autorotation of Unmanned Rotorcraft using Nonlinear Model Predictive Control," *J. of Intelligent and Robotic Systems*, Vol. 57, 2010, pp. 351369.

[46]Tierney, S. and Langelaan, J. W., "Autorotation Path Planning Using Backwards Reachable Set and Optimal Control," *Am. Helicopter Soc.*, 2010.

[47]Holsten, J., Loechelt, S., and Alles, W., "Autonomous Autorotation Flights of Helicopter UAVs to Known Landing Sites," *Am. Helicopter Soc.*, 2010.

[48]Yomchinda, T., Horn, J. F., and Langelaan, J. W., "Flight Path Planning for Descent-phase Helicopter Autorotation," *AIAA Guidance, Navigation, and Control Conf.*, 2011.

[49]Bryson, A. E. and Ho, Y. C., *Applied Optimal Control*, Taylor & Francis Group, New York, 1975.

[50]Kehoe, J. J., Watkins, A. S., and Lind, R., "A Time-Varying Hybrid Model for Dynamic Motion Planning of an Unmanned Air Vehicle," *AIAA Guidance, Navigation and Control Conf.*, 2006.

[51]Yakimenko, O., Xu, Y., and Basset, G., "Computing Short-Time Aircraft Maneuvers Using Direct Methods," *AIAA Guidance, Navigation, and Control Conf.*, 2008.

[52]Padfield, G. D., *Helicopter Flight Dynamics*, Blackwell Science Ltd, Oxford, UK, 1996.

[53]Chen, R. T. N., Lebacqz, J. V., Aiken, E. W., and Tischler, M. B., "Helicopter Mathematical Models and Control Law Development for Handling Qualities Research," Tech. Rep. NCR 2495, NASA Ames Research Center, 1988.

[54]Latombe, J. C., *Robot Motion Planning*, Kluwer Int. Series in Engineering and Computer Science, Mass., 1991.

[55]Li, Z. and (eds.), J. C., *Nonholonomic Motion Planning*, Kluwer Academic, Norwell, MA, 1993.

[56]Soueres, P. and Boissonnat, J., *Optimal Trajectories for Nonholonomic Mobile Robots. Robot Motion Planning and Control, edited by J. Laumond, Lecture Notes in Control and Information Sciences, pp. 93170*, Springer-Verlag, London, 1998.

[57]Kim, S. K. and Tilbury, D. M., "Trajectory Generation for a Class of Nonlinear Systems with Input and State Constraints," *Am. Control Conf.*, 2001.

[58]Gong, Q., Lewis, L. R., and Ross, I. M., "Pseudospectral Motion Planning for Autonomous Vehicles," *AIAA J. of Guidance, Control, and Dynamics*, Vol. 32, No. 3, 2009.

[59]Schouwenaars, T., Mettler, B., Legendre, P., and Dale, M. R. T., "Robust Motion Planning Using a Maneuver Automaton with Built-in Uncertainties," *Am. Control Conf.*, 2003.

[60]Murray, R. M., *Robust Control and nonholonomic motion planning*, Ph.D. thesis, University of California at Berkeley, 1990.

[61]Murray, R. M. and Sastry, S., "Nonholonomic Motion Planning: Steering Using Sinusoids," *IEEE Trans. on Automatic Control*, Vol. 38, 1993, pp. 700716.

[62]Skogestad, S. and Postlethwaite, I., *Multivariable Feedback Control: Analysis and Design, 2nd Ed.*, Wiley-Interscience, Great Britain, 2005.

[63]Kim, C. J., Sung, S. K., Park, S. H., Jung, S. N., and Yee, K., "Selection of Rotorcraft Models for Application to Optimal Control Problems," *AIAA J. of Guidance, Control, and Dynamics*, Vol. 31, No. 5, 2008.

[64]Ross, I. M., "Space Trajectory Optimization and L1-Optimal Control Problems," *Modern Astrodynamics - Elsevier Astrodynamics Series*, 2006, pp. 155–188.

[65]la Cour-Harbo, A. and Bisgaard, M., "State-Control Trajectory Generation for Helicopter Slung Load System using Optimal Control," *AIAA Guidance, Navigation, and Control Conf.*, 2009.

[66]Chen, R. T. N., "Flap-Lag Equations of Motion of Rigid, Articulated Rotor Blades with Three Hinge Sequences," Tech. Rep. NTM 100023, NASA Ames Research Center, 1987.

[67]Peters, D. A. and HaQuang, N., "Technical Notes - Dynamic Inflow for Practical Applications," *J. of the Am. Helicopter Soc.*, 1988, pp. 64–68.

[68]Peters, D. A. and He, C. J., "Finite State Induced Flow Models Part II: Three-Dimensional Rotor Disk," *AIAA J. of Aircraft*, Vol. 32, No. 2, 1995, pp. 323–333.

[69]Ardema, M. D. and Rajan, N., "Separation of Time Scales in Aircraft Trajectory Optimization," *J. of Guidance, Control, and Dynamics*, Vol. 8, No. 2, 1985, pp. 275278.

[70]ART, http://www.flightlab.com/, Mountain View CA., U.S.A.

[71]Taamallah, S., "Small-Scale Helicopter Blade Flap-Lag Equations of Motion For A Flybarless Pitch-Lag-Flap Main Rotor," *AIAA Modeling and Simulation Technologies Conf.*, 2011.

[72]Taamallah, S., "Flight Dynamics Modeling For A Small-Scale Flybarless Helicopter UAV," *AIAA Atmospheric Flight Mechanics Conf.*, 2011.

[73]Chen, R. T. N., "A Simplified Rotor System Mathematical Model for Piloted Flight Dynamics Simulation," Tech. Rep. NTM 78575, NASA Ames Research Center, 1979.

[74]Chen, R. T. N., "Effects of Primary Rotor Parameters on Flapping Dynamics," Tech. Rep. NTP 1431, NASA Ames Research Center, 1980.

[75]Pitt, D. M. and Peters, D. A., "Theoretical Prediction of Dynamic-Inflow Derivatives," *Europ. Rotorcraft Forum*, 1980.

[76]Leishman, G. J., *Principles of Helicopter Aerodynamics*, Cambridge University Press, Cambridge, UK, 2000.

[77]Johnson, W., *Helicopter Theory*, Dover Publications Inc., NY, USA, 1994.

[78]Bailey, F. J., "A Simplified Theoretical Method of Determining the Characteristics of a Lifting Rotor in Forward Flight," Tech. Rep. RNo. 716, NACA, 1941.

[79]Seckel, E. and Curtiss, H. C., "Aerodynamic Characteristics of Helicopter Rotors," Tech. Rep. No. 659, Department of Aerospace and Mechanical Engineering, Princeton University, 1962.

[80]Peters, D. A. and He, C., "Technical Note: Modification of Mass-Flow parameter to Allow Smooth Transition Between Helicopter and Windmill States," *J. of the Am. Helicopter Soc.*, 2006, pp. 275–278.

[81]Taamallah, S., "Low-Order Modeling For A Small-Scale Flybarless Helicopter UAV, A Grey-Box Time-Domain Approach," *AIAA Atmospheric Flight Mechanics Conf.*, 2012.

[82]Murray, R. M., "Nonlinear Control of Mechanical Systems: A Lagrangian Perspective," *Annual Reviews in Control*, Vol. 21, 1997, pp. 3145.

[83]Prouty, R. W., *Helicopter Performance, Stability, and Control*, Krieger Publishing Company, Malabar, Florida USA, 1995.

[84]Etkin, B. and Reid, L. D., *Dynamics of Flight: Stability and Control (3rd Ed.)*, John Wiley & Sons, U. S. A., 1996.

[85]Cooke, A. K. and Fitzpatrick, E. W. H., *Helicopter Test And Evaluation*, AIAA Education Series, Reston VA, USA, 2002.

[86]Menon, P. P., Bates, D. G., and Postlethwaite, I., "Computation of Worst-Case Pilot Inputs for Nonlinear Flight Control System Analysis," *AIAA J. of Guidance, Control, and Dynamics*, Vol. 29, No. 1, 2006, pp. 195–199.

[87]Goerzen, C., Kong, Z., and Mettler, B., "A Survey of Motion Planning Algorithms from the Perspective of Autonomous UAV Guidance," *J. Intell. Robot Syst.*, Vol. 57, 2010, pp. 65–100.

[88]Dadkhah, N. and Mettler, B., "Survey of Motion Planning Literature in the Presence of Uncertainty: Considerations for UAV Guidance," *J. Intell. Robot Syst.*, Vol. 65, 2012, pp. 233–246.

[89]Sundar, S. and Shiller, Z., "Optimal Obstacle Avoidance Based On The Hamilton-Jacobi-Bellman Equation," *IEEE Trans. on Robotics and Automation*, Vol. 13, No. 2, 1997, pp. 305–310.

[90]Schiller, Z., "On-Line Suboptimal Obstacle Avoidance," *IEEE Int. Conf. on Robotics and Automation*, 1999.

[91]Hagenaars, H. L., Imura, J., and Nijmeijer, H., "Approximate Continuous-Time Optimal Control in Obstacle Avoidance by Time/Space Discretization of Nonconvex State Constraints," *IEEE Int. Conf. on Control Applications*, 2004.

[92]Kim, H. J., Shim, D. H., and Sastry, S., "Nonlinear Model Predictive Tracking Control for Rotorcraft-Based Unmanned Aerial Vehicles," *Am. Control Conf.*, 2002.

[93]Patel, R. B. and Goulart, P. J., "Trajectory Generation for Aircraft Avoidance Maneuvers Using Online Optimization," *AIAA J. of Guidance, Control, and Dynamics*, Vol. 34, No. 1, 2011.

[94]Kolmogorov, A. N. and Fomin, S. V., *Elements of the Theory of Functions and Functional Analysis*, Dover Publications, N.Y., 1999.

[95]Lewis, L. P. R., "Rapid Motion Planning and Autonomous Obstacle Avoidance for Unmanned Vehicles," Tech. rep., Master Thesis, Naval Postgraduate School, 2006.

[96]Bliss, G. A., *Lectures on the Calculus of Variations*, University of Chicago Press, Chicago IL, 1946.

[97]Pontryagin, L. S., Boltyanskii, V. G., Gamkrelidze, R. V., Mishchenko, E. F., Trirogoff, K. N., and Neustadt, L. W., *Mathematical Theory of Optimal Processes*, Interscience, NY, 1962.

[98]Weinstock, R., *Calculus of Variations*, Dover Publications, NY, 1974.

[99]van Brunt, B., *The Calculus of Variations*, Springer-Verlag, NY, 2004.

[100]Vanderbei, R. J. and Shanno, D. F., "An Interior-Point Algorithm for Nonconvex Nonlinear Programming," *Computational Optimization and Applications*, Vol. 13, 1999, pp. 231–252.

[101]Byrd, R. H., Nocedal, J., and Waltz, R. A., "KNITRO: An Integrated Package for Nonlinear Optimization," *Large-Scale Nonlinear Optimization, Springer-Verlag*, 2006, pp. 35–59.

[102]Wachter, A., *An Interior Point Algorithm for Large-Scale Nonlinear Optimization with Applications in Process Engineering*, Ph.D. thesis, Carnegie-Mellon University, 2002.

[103]Wachter, A. and Biegler, L. T., "On the Implementation of an Interior-Point Filter Line-Search Algorithm for Large-Scale Nonlinear Programming," *Mathematical Programming*, Vol. 106, No. 1, 2006, pp. 25–57.

[104]Biegler, L. T. and Zavala, V. M., "Large-Scale Nonlinear Programming Using IPOPT: An Integrating Framework for Enterprise-Wide Optimization," *Computers and Chemical Engineering*, Vol. 33, 2008, pp. 575–582.

[105]Keller, H. B., "Numerical Solution of Two Point Boundary Value Problems," *SIAM*, 1976.

[106]Bock, H. G. and Plitt, K. J., "A Multiple Shooting Algorithm for Direct Solution of Optimal Control Problems," *IFAC 9th W.C.*, 1984.

[107]Stoer, J. and Bulirsch, R., *Introduction to Numerical Analysis*, Springer-Verlag, 2002.

[108]Reddien, G. W., "Collocation at Gauss Points as a Discretization in Optimal Control," *SIAM J. on Control and Optimization*, Vol. 17, No. 2, 1979, pp. 298306.

[109]Hargraves, C. R. and Paris, S. W., "Direct Trajectory Optimization Using Nonlinear Programming and Collocation," *AIAA J. of Guidance, Control, and Dynamics*, Vol. 10, No. 4, 1987.

[110]Enright, P. J. and Conway, B. A., "Discrete Approximations to Optimal Trajectories Using Direct Transcription and Nonlinear Programming," *AIAA J. of Guidance, Control, and Dynamics*, Vol. 15, No. 4, 1992.

[111]Hull, D., "Conversion of Optimal Control Problems into Parameter Optimization Problems," *AIAA J. of Guidance, Control, and Dynamics*, Vol. 20, No. 1, 1997, pp. 57–60.

[112]Biegler, L. T., "An Overview Of Simultaneous Strategies For Dynamic Optimization," *Chemical Engineering and Processing: Process Intensification*, Vol. 46, No. 11, 2007, pp. 1043–1053.

[113]Schwartz, A., *Theory and Implementation of Numerical Methods Based on Runge-Kutta Integration for Solving Optimal Control Problems*, Ph.D. thesis, University of California at Berkeley, 1996.

[114]Hager, W. W., "Runge-Kutta Methods in Optimal Control and the Transformed Adjoint System," *Numer. Math.*, Vol. 87, 2000, pp. 247282.

[115]Betts, J. T., "Practical Methods for Optimal Control Using Nonlinear Programming," *SIAM*, 2001.

[116]Betts, J. T., "Survey of Numerical Methods for Trajectory Optimization," *AIAA J. of Guidance, Control, and Dynamics*, Vol. 21, No. 2, 1998, pp. 193–207.

[117]Bottasso, C. L., Maisano, G., and Scorcelletti, F., "Trajectory Optimization Procedures for Rotorcraft Vehicles Including Pilot Models, with Applications to ADS-33 MTEs, Cat-A and Engine Off Landings," *Am. Helicopter Soc.*, 2009.

[118]Dickmanns, E. D. and Well, H., "Approximate Solution of Optimal Control Problems Using Third-Order Hermite Polynomial Functions," *6th Technical Conf. on Optimization Techniques*, 1975.

[119]Enright, P. J. and Conway, B. A., "Optimal Finite-Thrust Spacecraft Trajectories Using Collocation and Nonlinear Programming," *AIAA J. of Guidance, Control, and Dynamics*, Vol. 14, No. 5, 1991, pp. 981–985.

[120]Tang, S. and Conway, B., "Optimization of Low-Thrust Interplanetary Trajectories Using Collocation and Nonlinear Programming," *AIAA J. of Guidance, Control, and Dynamics*, Vol. 18, No. 3, 1995, pp. 599–604.

[121]Coverstone-Carroll, V. and Prussing, J. E., "Optimal Cooperative Power-Limited Rendezvous With Propellant Constraints," *J. of the Astronautical Sciences*, Vol. 43, No. 3, 1995, pp. 289–305.

[122]Herman, A. L. and Conway, B. A., "Direct Optimization Using Collocation Based on High-Order Gauss-Lobatto Quadrature Rules," *AIAA J. of Guidance, Control, and Dynamics*, Vol. 19, No. 3, 1996, pp. 592–599.

[123]Roh, W. and Kim, Y., "Trajectory Optimization for a Multi-Stage Launch Vehicle Using Time Finite Element and Direct Collocation Methods," *Engineering Optimization*, Vol. 34, No. 1, 2002, pp. 15–32.

[124]Hoffren, J. and Raivio, T., "Optimal Maneuvering After Engine Failure," *AIAA Atmospheric Flight Mechanics Conf.*, 2000.

[125]Hyde, D. C., "Minimum-Altitude-Loss Gliding Turns With Terminal Constraints (Return to Runway After Engine Failure)," *AIAA Atmospheric Flight Mechanics Conf.*, 2005.

[126]Brinkman, K. and Visser, H. G., "A closed-loop guidance approximation for the turn-back maneuver after engine failure during climb-out," *45th AIAA Aerospace Sciences Meeting and Exhibit*, 2007.

[127]Geiger, B. R., Horn, J. F., Sinsley, G. L., Ross, J. A., Long, L. N., and Niessner, A. F., "Flight Testing a Real-Time Direct Collocation Path Planner," *AIAA J. of Guidance, Control, and Dynamics*, Vol. 31, 2008, pp. 1575–1586.

[128]Misovec, K., Inanc, T., Wohletz, J., and Murray, R. M., "LowObservable Nonlinear Trajectory Generation for Unmanned Air Vehicles," *IEEE Conf. on Decision and Control*, 2003.

[129]Zhao, Y. J. and Qi, Y. C., "Minimum Fuel Powered Dynamic Soaring of Unmanned Aerial Vehicles Utilizing Wind Gradients," *Optimal Control Applications and Methods*, Vol. 25, No. 5, 2004, pp. 211233.

[130]Borrelli, F., Subramanian, D., Raghunathan, A. U., and Biegler, L. T., "MILP and NLP Techniques for Centralized Trajectory Planning of Multiple Unmanned Air Vehicles," *Am. Control Conf.*, 2006.

[131]Zhao, Y. J., "Optimal Patterns of Glider Dynamic Soaring," *Opt. Ctrl. App. and Meth.*, Vol. 25, No. 2, 2004, pp. 6789.

[132]Dontchev, A. L., Hager, W. W., and Veliov, V. M., "Second-Order Runge-Kutta Approximations In Constrained Optimal Control," *SIAM J. on Numerical Analysis*, Vol. 38, 2000, pp. 202226.

[133]Dontchev, A. L., Hager, W. W., and Veliov, V. M., "Uniform Convergence and Mesh independence of Newtons method for Discretized Variational Problems," *SIAM J. on Control and Optimization*, Vol. 39, 2000, pp. 961980.

[134]Cuthrell, J. E. and Biegler, L. T., "Simultaneous Optimization and Solution Methods for Batch Reactor Control Profiles," *Computers and Chemical Engineering*, Vol. 13, No. 12, 1989, pp. 4962.

[135]Kameswaran, S. and Biegler, L. T., "Convergence Rates for Direct Transcription of Optimal Control Problems at Radau Points," *Am. Control Conf.*, 2006.

[136]Elnagar, J., Kazemi, M. A., and Razzaghi, M., "The Pseudospectral Legendre Method for Discretizing Optimal Control Problems," *IEEE Trans. on Automatic Control*, Vol. 40, No. 10, 1995, pp. 17931796.

[137]Fahroo, F. and Ross, I. M., "Direct Trajectory Optimization by a Chebyshev Pseudospectral Method," *J. of Guidance, Control, and Dynamics*, Vol. 25, No. 1, 2002.

[138]Benson, D. A., Huntington, G. T., Thorvaldsen, T. P., and Rao, A. V., "Direct Trajectory Optimization and Costate Estimation via an Orthogonal Collocation Method," *AIAA J. of Guidance, Control, and Dynamics*, Vol. 29, No. 6, 2006.

[139]Fahroo, F. and Ross, I. M., "Pseudospectral Methods for Infinite Horizon Nonlinear Optimal Control Problems," *AIAA Guidance, Navigation and Control Conf.*, 2005.

[140]Garg, D., Patterson, M. A., Darby, C. L., Francolin, C., Huntington, G. T., Hager, W. W., and Rao, A. V., "Direct Trajectory Optimization and Costate Estimation of General Optimal Control Problems Using a Radau Pseudospectral Method," *AIAA Guidance Navigation and Control Conf.*, 2009.

[141]Darby, C. L., Hager, W. W., and Rao, A. V., "Direct Trajectory Optimization Using a Variable Low-Order Adaptive Pseudospectral Method," *AIAA J. of Spacecraft and Rockets*, Vol. 48, No. 3, 2011.

[142]Ross, I. M. and Fahroo, F., "Pseudospectral Methods for Optimal Motion Planning of Differentially Flat Systems," *IEEE Trans. on Automatic Control*, Vol. 49, No. 8, 2004, pp. 1410–1413.

[143]Gong, Q., Kang, W., and Ross, I. M., "A Pseudospectral Method for the Optimal Control of Constrained Feedback Linearizable Systems," *IEEE Trans. on Automatic Control*, Vol. 51, No. 7, 2006.

[144]Rao, A. V., "A Survey of Numerical Methods for Optimal Control," *Am. Astronautical Soc.*, 2009.

[145]Fahroo, F. and Ross, I. M., "Second Look at Approximating Differential Inclusions," *AIAA J. of Guidance, Control, and Dynamics*, Vol. 24, No. 1, 2001.

[146]Fornberg, B., *A Practical Guide to Pseudospectral Methods*, Cambridge University Press, 1998.

[147]Dai, R. and Cochran, J. E., "Wavelet Collocation Method for Optimal Control Problems," *J. Optim. Theory Appl.*, Vol. 143, 2009, pp. 265278.

[148]Davis, P. J. and Rabinowitz, P., *Methods of Numerical Integration*, Dover Publications, 2007.

[149]Vlassenbroeck, J. and Doreen, R. V., "Chebyshev Technique for Solving Nonlinear Optimal Control Problems," *IEEE Trans. on Automatic Control*, Vol. 33, No. 4, 1988, pp. 333340.

[150]Huntington, G. T., Benson, D. A., and Rao, A. V., "A Comparison of Accuracy and Computational Efficiency of Three Pseudospectral Methods," *AIAA Guidance, Navigation, and Control Conf.*, 2007.

[151]Neuman, C. P. and Sen, A., "A Suboptimal Control Algorithm for Constrained Problems using Cubic Splines," *Automatica*, Vol. 9, 1973, pp. 601–613.

[152]Lu, P., Sun, H., and Tsai, B., "Closed-Loop Endoatmospheric Ascent Guidance," *AIAA J. of Guidance, Control and Dynamics*, Vol. 26, No. 2, 2003, pp. 283–294.

[153]Rea, J., "Launch Vehicle Trajectory Optimization Using a Legendre Pseudospectral Method," *AIAA Guidance, Navigation, and Control Conf.*, 2003.

[154]Josselyn, S. and Ross, I. M., "Rapid Verification Method for the Trajectory Optimization of Reentry Vehicles," *AIAA J. of Guidance, Control, and Dynamics*, Vol. 26, No. 3, 2003.

[155]Williams, P., "Application of Pseudospectral Methods for Receding Horizon Control," *AIAA J. of Guidance, Control, and Dynamics*, Vol. 27, No. 2, 2004, pp. 310–314.

[156]Infeld, S. I., *Optimization of Mission Design for Constrained Libration Point Space Missions*, Ph.D. thesis, Stanford University, 2005.

[157]Riehl, J. P., Paris, S. W., and Sjaw, W. K., "Comparision of Implicit Integration Methods for Solving Aerospace Trajectory Optimization Problems," *AIAA/AAS Astrodynamics Specialists Conf.*, 2006.

[158]Hawkins, A. M., Fill, T. R., Proulx, R. J., and Feron, E. M., "Constrained Trajectory Optimization for Lunar Landing," *AAS Spaceflight Mechanics Meeting*, 2006.

[159]Bollino, K. P., Lewis, L. R., Sekhavat, P., and Ross, I. M., "Pseudospectral Optimal Control: A Clear Road for Autonomous Intelligent Path Planning," *AIAA Infotech*, 2007.

[160]Bedrossian, N., Bhatt, S., Lammers, M., Nguyen, L., and Zhang, Y., "First Ever Flight Demonstration of Zero Propellant Maneuver TM Attitude Control Concept," *AIAA Guidance, Navigation, and Control Conf.*, 2007.

[161]Gong, Q., Wei, K., Bedrossian, N. S., Fahroo, F., Sekhavat, P., and Bollino, K., "Pseudospectral Optimal Control for Military and Industrial Applications," *IEEE Conf. on Decision and Control*, 2007.

[162]Ross, I. M., Sekhavat, P., Fleming, A., and Gong, Q., "Optimal Feedback Control: Foundations, Examples, and Experimental Results for a New Approach," *AIAA J. of Guidance, Control, and Dynamics*, Vol. 31, No. 2, 2008.

[163]Karpenko, M., Bhatt, S., Bedrossian, N., Fleming, A., and Ross, I. M., "Flight Implementation of Pseudospectral Optimal Control for the TRACE Space Telescope," *AIAA Guidance, Navigation and Control Conf.*, 2011.

[164]Ceriotti, M. and McInnes, C. R., "Generation of Optimal Trajectories for Earth Hybrid Pole Sitters," *AIAA J. of Guidance, Control, and Dynamics*, Vol. 34, No. 3, 2011, pp. 847–859.

[165]Yan, H., Gong, Q., Park, C. D., Ross, I. M., and Souza, C. N. D., "High-Accuracy Trajectory Optimization for a Trans-Earth Lunar Mission," *AIAA J. of Guidance, Control, and Dynamics*, Vol. 34, No. 4, 2011, pp. 1219–1227.

[166]Darby, C. L. and Rao, A. V., "Minimum-Fuel Low-Earth-Orbit Aeroassisted Orbital Transfer of Small Spacecraft," *AIAA J. of Spacecraft and Rockets*, Vol. 48, No. 4, 2011.

[167]Boyarko, G., Yakimenko, O., and Romano, M., "Optimal Rendezvous Trajectories of a Controlled Spacecraft and a Tumbling Object," *AIAA J. of Guidance, Control, and Dynamics*, Vol. 34, No. 4, 2011, pp. 1239–1252.

[168]Boyarko, G., Romano, M., and Yakimenko, O., "Time-Optimal Reorientation of a Spacecraft Using an Inverse Dynamics Optimization Method," *AIAA J. of Guidance, Control, and Dynamics*, Vol. 34, No. 4, 2011, pp. 1197–1208.

[169]Zhang, K. and Chen, W., "Reentry Vehicle Constrained Trajectory Optimization," *AIAA Int. Space Planes and Hypersonic Systems and Technologies*, 2011.

[170]Paris, S. W., Riehl, J. P., and Sjaw, W. K., "Enhanced Procedures for Direct Trajectory Optimization Using Nonlinear Programming and Implicit Integration," *AIAA/AAS Astrodynamics Specialists Conf.*, 2006.

[171]Cottrill, G. C. and Harmon, F. G., "Hybrid Gauss Pseudospectral and Generalized Polynomial Chaos Algorithm to Solve Stochastic Trajectory Optimization Problems," *AIAA Guidance Navigation and Control Conf.*, 2011.

[172]Dekel, M. and Ben-Asher, J. Z., "Pseudo-Spectral-Method Based Optimal Glide in the Event of Engine Cut-off," *AIAA Guidance, Navigation, and Control Conf.*, 2011.

[173]Dai, R. and Cochran, J. E., "Three-Dimensional Trajectory Optimization in Constrained Airspace," *AIAA J. of Aircraft*, Vol. 46, No. 2, 2009, pp. 627634.

[174]Hartjes, S., Visser, H. G., and Pavel, M. D., "Environmental Optimization Of Rotorcraft Approach Trajectories," *Europ. Rotorcraft Forum*, 2011.

[175]Harada, M. and Bollino, K., "Optimal Trajectory of a Glider in Ground Effect and Wind Shear," *AIAA Guidance, Navigation and Control Conf.*, 2005.

[176]McCracken, B. D., Burzota, K. L., Ramos, M. M., and Jorris, T. R., "Cooperative Unmanned Air Vehicle Mission Planning and Collision Avoidance," *AIAA Infotech*, 2011.

[177]Choe, R. and Hovakimyan, N., "Perching Maneuver for an MAV Augmented with an L1 Adaptive Controller," *AIAA Guidance, Navigation, and Control Conf.*, 2011.

[178]Harada, M. and Bollino, K., "Minimum-Time Circling Flight of a Triarm Coaxial Rotor UAV," *AIAA Guidance Navigation and Control Conf.*, 2011.

[179]GPOPS, http://www.gpops.org/, U.S.A.

[180]Huntington, G. T. and Rao, A. V., "Comparison of Global and Local Collocation Methods for Optimal Control," *AIAA J. of Guidance, Control, and Dynamics*, Vol. 31, No. 2, 2008.

[181]Rao, A. V., Benson, D. A., Darby, C., Patterson, M. A., Francolin, C., Sanders, I., and Huntington, G. T., "Algorithm xxx: GPOPS, A MATLAB Software for Solving Multiple-Phase Optimal Control Problems Using the Gauss Pseudospectral Method," Tech. rep., ACM Inc., 2008.

[182]Ross, I. M. and Fahroo, F., "A Direct Method for Solving Nonsmooth Optimal Control Problems," *IFAC 15th Triennial World Congress*, 2002.

[183]Pegg, R. J., "An Investigation of the Helicopter Height-Velocity Diagram Showing Effects of Density Altitude and Gross Weight," Tech. Rep. TN D-4536, NASA Langley Research Center, 1968.

[184]Katzenberger, E. F. and Rich, M. J., "An Investigation of Helicopter Descent and Landing Characteristics Following Power Failure," *J. of Aeron Sci*, Vol. 23, No. 4, 1956, pp. 345–356.

[185]Jepson, W. D., "Some Considerations of the Landing and Take-Off Characteristics of Twin Engine Helicopters. Part I - Height-Velocity and Part Power Descents," *J. of the Am. Helicopter Soc.*, Vol. 7, No. 4, 1962, pp. 33–37.

[186]Hanley, W. J. and DeVore, G., "An Analysis of the Helicopter Height-Velocity Diagram Including a Practical Method for Its Determination," Tech. Rep. ADS 67-23, FAA, 1967.

[187]Besse, J. M., "The Unsafe Zone for Single Engine Helicopters," *Europ. Rotorcraft Forum*, 1978.

[188]Wood, T. L., "High Energy Rotor Systems," *Am. Helicopter Soc.*, 1976.

[189]Dooley, L. W. and Yeary, R. D., "Flight Test Evaluation of the High Inertia Rotor System," Tech. Rep. UARTL-TR-79-9, U.S. Army Research and Technology Laboratories (AVRADCOM), 1979.

[190]Szymanowski, M. K., "Improving Helicopter Height-Velocity Performance," *Europ. Rotorcraft Forum*, 1999.

[191]Schillings, J., McCollough, J., Hollifield, P., Wasylyszyn, J., and Grife, R., "Height-Velocity Testing of a Growth Rotor for the Bell 407 Aircraft," *Am. Helicopter Soc.*, 2007.

[192]Kim, C. J., Park, S. H., Sung, S. K., and Jung, S. N., "Nonlinear Optimal Control Analysis Using State-Dependent Matrix Exponential and Its Integrals," *AIAA J. of Guidance, Control, and Dynamics*, Vol. 32, No. 1, 2009.

[193]Elnagar, J. and Kazemi, M. A., "Pseudospectral Legendre-based Optimal Computation of Nonlinear Constrained Variational Problems," *J. of Computational and Applied Mathematics*, Vol. 88, 1997, pp. 363–375.

[194]Rao, A. V., "Extension of a Pseudospectral Legendre Method to Non-Sequential Multiple-Phase Optimal Control Problems," *AIAA Guidance, Navigation, and Control Conf.*, 2003.

[195]Ross, I. M., Gong, Q., and Sekhavat, P., "The Bellman Pseudospectral Method," *AIAA/AAS Astrodynamics Specialist Conf.*, 2008.